

Review

Framework-Enhanced Electrochemiluminescence in Biosensing

Haomin Fu, Zhiyuan Xu, Hanlin Hou, Rengan Luo, Huangxian Ju and Jianping Lei * 

State Key Laboratory of Analytical Chemistry for Life Science, School of Chemistry and Chemical Engineering, Nanjing University, Nanjing 210023, China; hxju@nju.edu.cn (H.J.)

* Correspondence: jpl@nju.edu.cn

Abstract: Electrochemiluminescence (ECL) has attracted increasing attention owing to its intrinsic advantages of high sensitivity, good stability, and low background. Considering the fact that framework nanocrystals such as metal–organic frameworks and covalent organic frameworks have accurate molecular structures, a series of framework-based ECL platforms are developed for decoding emission fundamentals. The integration of fluorescent ligands into frameworks significantly improves the ECL properties due to the arrangement of molecules and intramolecular electron transfer. Moreover, the various framework topologies can be easily functionalized with the recognition elements to trace the targets for signal readout. These ECL enhancement strategies lead to a series of sensitive analytical methods for protein biomarkers, DNA, small biomolecules, and cells. In this review, we summarize recent advances in various functions of frameworks during the ECL process, and constructions of framework-based ECL platforms for biosensing. The framework-based ECL nanoemitters and enhancement mechanisms show both theoretical innovation and potential applications in designing ECL biosensing systems. Perspectives are also discussed, which may give a guideline for researchers in the fields of ECL biosensing and reticular materials.

Keywords: electrochemiluminescence; frameworks; biosensing; nanoemitters



Citation: Fu, H.; Xu, Z.; Hou, H.; Luo, R.; Ju, H.; Lei, J. Framework-Enhanced Electrochemiluminescence in Biosensing. *Chemosensors* **2023**, *11*, 422. <https://doi.org/10.3390/chemosensors11080422>

Academic Editor: Christos Kokkinos

Received: 28 June 2023

Revised: 23 July 2023

Accepted: 25 July 2023

Published: 28 July 2023



Copyright: © 2023 by the authors. Licensee MDPI, Basel, Switzerland. This article is an open access article distributed under the terms and conditions of the Creative Commons Attribution (CC BY) license (<https://creativecommons.org/licenses/by/4.0/>).

1. Introduction

Electrochemiluminescence (ECL) is a classic and powerful analytical technique involving a redox process at electrodes where excited states are electrochemically generated and emit light [1,2]. Benefitting from its unique light-free luminescence mechanism, ECL has many advantages for an analysis, such as a high sensitivity, good stability, and low background [3]. Nowadays, ECL is widely applied in the areas of environmental monitoring [4], cell sensing [5], imaging [6], food [7], and water safety [8]. ECL-driven tumor photodynamic therapy (PDT) was proposed through the effective energy transfer from ECL emission to photosensitizer chlorin e6 [9]. With a high spatiotemporal controllability, stable luminescence, and high photon flux of ECL, ECL microscopy may be more fascinating than fluorescence [10], bioluminescence [11], and surface-enhanced Raman scattering [12]. Over several decades of research, the variety of ECL emitters has substantially increased, and they can be broadly classified into an inorganic system (such as Ir or Ru complexes), an organic system (such as luminols), and semiconductor nanomaterials [13]. Recently, several novel nanomaterials have been used as luminophores in ECL, such as Au nanomaterials [14], quantum dots [15], and frameworks [16]. The combinations of ECL techniques and these new materials broaden the scope of ECL applications.

Frameworks containing metal–organic frameworks (MOFs), covalent–organic frameworks (COFs), and hydrogen-bonded organic frameworks (HOFs) have been developed rapidly since the 21st century [17,18]. Owing to their flexible, synthetically controllable, and adjustable structure, frameworks have been utilized in various areas such as energy storage, sewage treatment, gas separation, catalysis, and biosensing [19]. Although there are some deficiencies for electrochemical reactions in frameworks, such as an intrinsic poor electroconductivity and low mass permeability [20], frameworks have been gradually

regarded as one of the most promising nanomaterials in ECL assays. Different from other ECL luminophores like metal complexes and quantum dots, predesignable structures of frameworks make them more suitable and efficient in ECL processes. For example, Yin's group designed an ECL-active MOF by using a ruthenium complex as a ligand and more intense ECL emission was observed with the aid of graphene oxide [21]. By combining a predesigned structure with post-modification, frameworks provide various strategies to regulate their ECL signals for adapting the requirement. Furthermore, the structures of frameworks are utilized dexterously to create novel ECL enhancement mechanisms for developing sensitive and stable analytical methods. Overall, the variation of an ECL signal highly depends on the optoelectronic properties of frameworks, which are adjustable with designation or post-modification [22].

In order to design self-luminescent reticular nanoemitters, three types of methods have been developed. First, frameworks can be synthesized with ECL-active luminophore ligands, such as porphyrin [23], pyrene [24], and aggregation-induced emission luminogen [25], for constructing emitters with an improved ECL efficiency. Second, the doping of transition metal elements is a promising way to deal with an intrinsic low conductivity of MOFs in ECL reactions. Classic Ru complexes [26] and novel lanthanide ions [27] are already applied in biosensing with this method. Third, non-emitting monomers can be endowed with intense ECL emission through a rational design. Typically, by utilizing well-designed donor/acceptor units, a high ECL efficiency of COFs could be realized [28,29].

Therefore, integrating the frameworks and ECL methods is of great significance to construct high-performance biosensing platforms. In recent years, the roles of frameworks in ECL processes develop rapidly with multifunctions in biosensing. Initially, frameworks were used as carriers of classic luminophores or catalysts to accelerate the ECL reactions, but they later became ECL emitters for biosensing platform establishment, achieving a successful analysis of proteins, nucleic acids, small molecules, and cells.

In this review, the various functions of frameworks in ECL emission are first analyzed to show the rapid development in this area (Figure 1). Then, framework-enhanced ECL biosensing applications in recent years are introduced and analyzed. Finally, perspectives and potential issues are proposed, which may guide the great development of framework-based ECL biosensing systems.

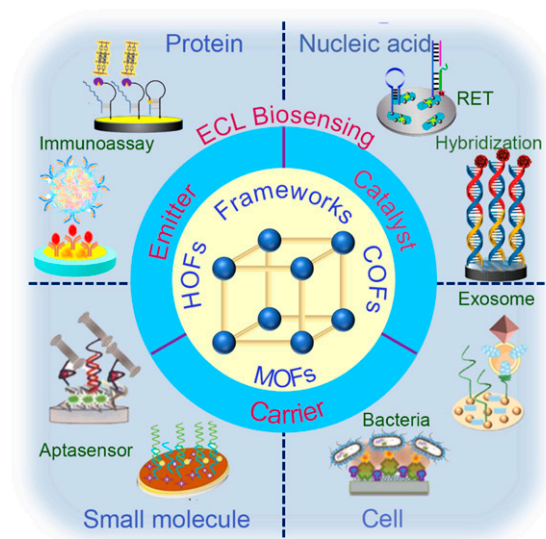


Figure 1. Schematic illustration of roles of frameworks in ECL processes and their ECL applications in biosensing.

2. The Roles of Frameworks in ECL Processes

Although the combination of frameworks with ECL demonstrates great potentials in signal readout, low conductivities and inert electrochemical properties of frameworks may

result in a poor sensing performance. Therefore, frameworks were often used as a carrier of efficient ECL emitters like quantum dots (QDs) or Ru complexes, or a catalyst to strengthen ECL emission during the initial period. After the report of the electroactive MOF [16], frameworks gradually began to be used as emitters in ECL processes and various ECL-active frameworks were extensively applied in biosensing with several emerging signal amplification strategies.

2.1. The Carriers of ECL Luminophores

The outstanding features of frameworks, such as an adjustable reticular structure, large surface area, tunable pore sizes, and functionalized sites, make them competent to be used as a carrier. In early reports, classic ECL luminophores (Ru complexes, luminol, QDs, et al.) were integrated with frameworks using encapsulation or post-modifications.

The encapsulation of ECL luminophores into frameworks is a widely applied strategy to make frameworks better in an ECL performance. Through introducing guest materials, host frameworks receive an improved ECL efficiency while largely maintaining their own original properties. Therefore, encapsulation gives a flexible way to prepare frameworks with promising ECL activity. In view of the porous structure of frameworks, Qin et al. prepared $\text{Ru}(\text{bpy})_3^{2+}$ -functionalized MOF thin films using the self-assembly approach (Figure 2a). Plenty of $\text{Ru}(\text{bpy})_3^{2+}$ molecules in Ru-MOF films showed an intense ECL emission and excellent behavior in the detection of the human-heart-type fatty-acid-binding protein [30]. Also, classic luminol-based frameworks are conducted through this method. Tang et al. synthesized porous Zn-based MOF, which loaded a large amount of luminol by encapsulating into its pores. The resulting Zn-MOF@luminol as the signal probe achieved a strong ECL signal for detecting concanavalin A [31]. Furthermore, luminophores with large sizes, such as QDs or $\text{g-C}_3\text{N}_4$, can be encapsulated in frameworks with high surface areas. As shown in Figure 2b, Fe-MIL-88B- NH_2 @ZnSe was successfully prepared via the one-pot method. By using Fe-MIL-88B- NH_2 as an efficient coreaction accelerator, the biosensor realized the sensitive detection of a squamous cell carcinoma antigen in human serum [32]. Qin et al. designed a triethanolamine-functionalized MOF on graphene oxide nanosheets to accomplish creating a rapid label-free ECL immunosensor for the detection of human copeptin [33].

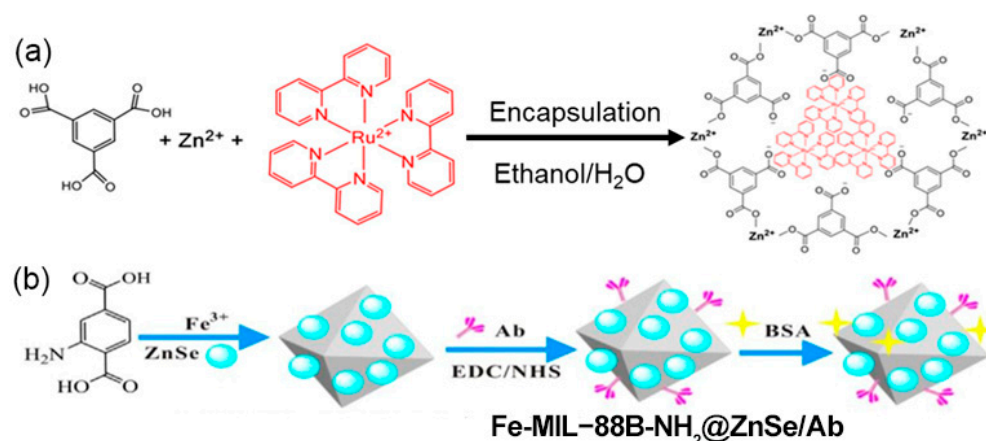


Figure 2. (a) Schematic diagram of the synthesis of $(\text{Ru}(\text{bpy})_3^{2+})$ -functionalized MOF (Ru-MOF). Reproduced from [30] with permission from the American Chemical Society. (b) Illustration for the construction of Fe-MIL-88B- NH_2 @ZnSe/Ab. Reproduced from [32] with permission from Elsevier.

On the basis of porosity and a large surface area, frameworks are considered to be suitable for post-modification with functional materials to obtain specific properties [34], which can be conducted through covalent or noncovalent bonding. For example, Wang et al. combined zeolitic imidazolate frameworks and luminol-capped Ag nanoparticles to form a luminol-AgNPs@ZIF-67 system via electrostatic interaction, which had ~115-fold-enhanced ECL compared to the luminol system [35]. In addition, QDs were merged onto MIL-53

through noncovalent adsorption and the resulting MIL-53@QDs platform demonstrated a large ECL intensity enhanced by the surface plasmon resonance process between AuNPs and CdS QDs for kanamycin and neomycin biosensing [36]. Furthermore, Liu's group developed a nanoreactor based on Ru(bpy)₃²⁺-doped nanoporous zeolite nanoparticles (Ru@zeolite) [37], in which frameworks not only served as a carrier of Ru complexes through post-modification but were also spatially confined for efficient collision reactions in situ ECL reactions.

2.2. The Catalyst in ECL Processes

By integrating catalytically active components, frameworks have been utilized as electrocatalysts, such as in an oxygen reduction reaction and CO₂ reduction, for a long time [38,39]. A more intense ECL emission will be observed when decisive elementary reactions are accelerated during the ECL process. For instance, Zn tetrakis(carboxyphenyl)-porphyrin (TCPP) linkers in MOF-525 acted as ECL active centers to facilitate the conversion from dissolved oxygen to singlet oxygen for enhanced ECL (Figure 3a). Based on MOF-525-Zn as signal amplifying probes, an ultrasensitive ECL sensor was proposed for the detection of protein kinase A activity with a linear range from 0.01 to 20 U mL⁻¹ and detection limit of 0.005 U mL⁻¹ [40]. Furthermore, the inorganic Zr–O clusters of MOF-525 simultaneously served as the recognition sites of phosphate groups for a specific bioanalysis.

On the other hand, MOFs were utilized as a coreactant accelerator to enhance the ECL of CdTe QDs through accelerating the generation of the sulfate radical anion (SO₄^{•-}), which is critical in producing excited states of QDs, further realizing an ultrasensitive bioanalysis of the cardiac troponin-I antigen [41]. Similarly, 2D Fe-Zr metal–organic layers were applied for the construction of an ECL immunosensor by utilizing their peroxidase-like activity, which could effectively enhance the ECL signal of luminol through H₂O₂ catalysis [42]. Additionally, Song et al. designed a signal-amplified ECL sensor chip via the synergistic catalysis of Au–Pd bimetallic nanocrystals and mixed-valence Ce-based MOFs for the fast reduction of dissolved O₂ (Figure 3b). By integrating a three-electrode detection system into the self-assembled microfluidic chip, the developed sensor showed a high sensitivity for procalcitonin detection with the automation and portability of the detection process [43]. In a word, by introducing active catalytic sites or utilizing intrinsic properties, frameworks have nanozyme-like functions for ECL catalytic enhancement.

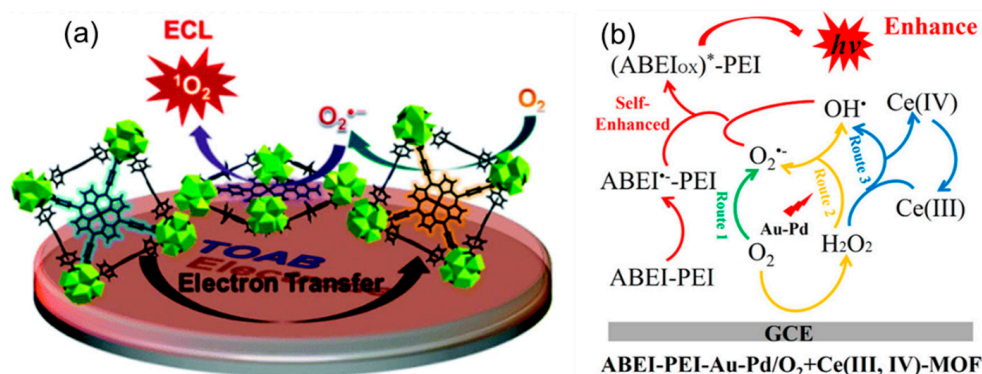


Figure 3. (a) Schematic illustration for the ECL catalysis mechanism of singlet oxygen based on MOF-525. Reproduced from [40] with permission from the Royal Society of Chemistry. (b) Supposed ECL catalysis mechanism for Au–Pd/O₂ + Ce(III, IV)-MOF system. “*” represents the excited state. Reproduced from [43] with permission from the American Chemical Society.

2.3. ECL Nanoemitters

Considering the structures of framework units, introducing ECL luminophores as linkers is thought to be a proper approach to establish framework-based ECL emitters. Due to intrinsic structural features, framework-based emitters are considered to be promising material for ECL biosensing based on the combined advantages of framework emitters and

ECL techniques [44]. Because of efficient energy migration [45], Ru-complex-based linkers have been applied for designing ECL-active frameworks since 2010. Ru(II) bipyridine ($\text{Ru}(\text{bpy})_3^{2+}$) derivatives as ligands can be synthesized into frameworks using coordination with metal ions or clusters [46]. For example, functionalized Ru-based MOF nanosheets comprising carboxyl-rich tris(4,4'-dicarboxylic acid-2,2'-bipyridyl) Ru(II) and Zn^{2+} nodes exhibited a good water solubility and excellent ECL performance (Figure 4a). By employing Ru-MOF as an ECL probe, a “signal-on” ECL immunosensor was designed for the selective detection of cardiac troponin I in the range from 1 fg/mL to 10 ng/mL [47]. However, Ru complexes are costly when adjusting their structures and large in steric size, which inevitably restrict their application in direct framework synthesis. In fact, Ru complexes are more often modified onto frameworks through a post-synthesized route, which makes frameworks work like a carrier rather than a nanoemitter [48,49]. Meanwhile, other ECL-active organic ligands, such as a porphyrin derivative, perylene-3,4,9,10-tetracarboxylate, and 9,10-anthracene dibenzoate (DPA), were utilized in constructing MOF emitters for proprotein convertase subtilisin/kexin type 9, microRNAs, and MCU1 detection, respectively [50–52].

Inspired by aggregation-induced emission (AIE) luminophores, which show a stronger photoluminescence in the aggregated state than that of the isolated one [53,54], frameworks constructed with AIE molecules become attractive in ECL sensing. Typically, tetraphenylethylene (TPE)-based AIEgens are mostly reported in recent research thanks to designable molecular structures. For instance, a fiber-like MOF, synthesized with the coordination of Zn^{2+} and 1,1,2,2-tetrakis(4-(pyridin-4-yl)phenyl)ethane (TPPE), showed a more intense ECL emission than its ligand TPPE in the presence of 1,4-diazabicyclo[2.2.2]octane (DABCO) (Figure 4b,c). More significantly, different from the constant ECL intensity using a tri-*n*-propylamine (TPrA) coreactant, DABCO exhibited a time-dependent ECL intensity due to the intrarecticular electron transfer through coordination interaction between DABCO and Zn^{2+} [55]. In another work, Wei's group synthesized a dumbbell-plate-shaped MOF consisting of 1,1,2,2-tetra(4-carboxylbiphenyl)ethylene and Zr(IV) cations, which was utilized as an ECL tag for neuron-specific enolase detection with a sandwich-type immunoreaction [56]. In addition, a two-dimensional AIEgen-based MOF was also fabricated into an efficient ECL biosensing platform [57], which restricted the intramolecular free rotation and vibration of these ligands and then reduced the non-radiative transition. The combination of AIE ligands and frameworks paved a potential way for better ECL sensors; that is, the large surface area and porous properties of MOFs make ECL reactions more effective while the AIE molecular motion is restricted by the rigid MOF structure, which is theoretically beneficial to AIE emission [58]. Similar to the term aggregation-induced emission, the strong ECL emission based on the restricted AIE molecules within MOFs has been named ‘aggregation-induced ECL’ (AIECL) [59], which is also successfully used in COFs [60] and polymers [61].

Identically, luminophores can be introduced into frameworks by serving as ion nodes. Due to a good photoluminescent emission and successful applications in biosensing [62], self-luminescent lanthanide MOFs (Ln-MOFs) are considered promising luminophores in ECL reactions. Dai's group synthesized La^{3+} -BTC MOFs as an ECL emitter and highly active reactor simultaneously to construct a gene sensor. With the assistance of crystal violet, a good performance toward a p53 gene analysis was obtained through the co-quenching effect mechanism [63]. Furthermore, Eu-based Ln-MOFs were prepared with 5-boronoisophthalic acid and Eu (III) ions. The ECL emission mechanism was identified to be that 5-bop was excited with ultraviolet photons to generate a triplet state, which then triggered Eu (III) ions for red emission. The Eu-MOFs showed a great sensitivity in an ECL immunoassay for Cytokeratin 21-1 detection [64].

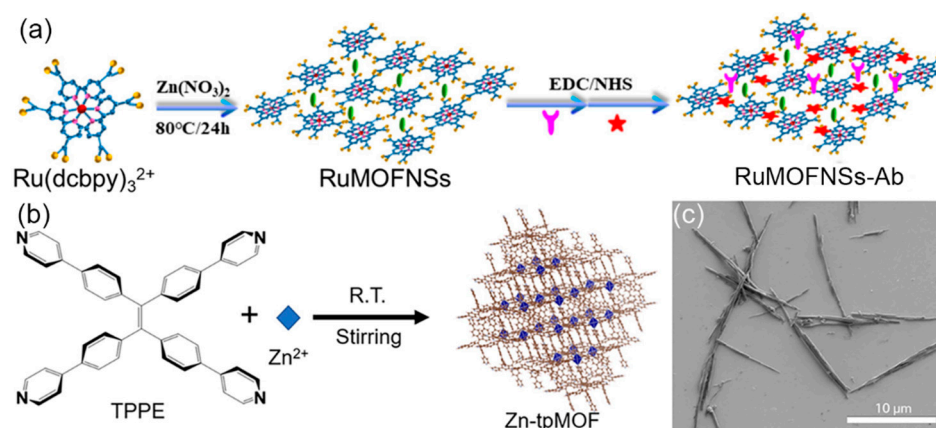


Figure 4. (a) Schematic illustration for the fabrication process of a Ru-MOF nanosheet. Reproduced from [47] with permission from the American Chemical Society. (b) The synthesis of and (c) SEM image of Zn-tpMOF. Reproduced from [55] with permission from Elsevier.

In order to obtain a better biosensing performance, a higher ECL efficiency is urgently needed. Conventional coreactant ECL is convenient in operation but inefficient in electron transfer due to the intermolecular route. Thanks to a shortened pathway of mass transport and electron transfer, the intramolecular electron transfer process is recognized as a promising solution [65]. Inspired by this theory, a mixed-ligand MOF (m-MOF) was designed for proof of concept by integrating it with two ligands, one as a luminophore and the other as a coreactant, on one metal node for self-enhanced ECL [66]. As shown in Figure 5a,b, the resulting m-MOF had a highly ordered crystalline unit proved by comparing the experimental PXRD pattern and theoretical simulation. Then, the m-MOF exhibited greatly enhanced ECL compared to its ligand and Zn-DPA MOF, indicating a high efficiency of the intrareticular charge transfer process (Figure 5c). Finally, the proposed stepwise ECL mechanism of the m-MOF was given as a result of local excitation in the DPA unit, which was identified through a density functional theory calculation (Figure 5d). Overall, the mixed-ligand approach successfully shortens the pathway of charge transfer, providing a new idea in ECL platform designs.

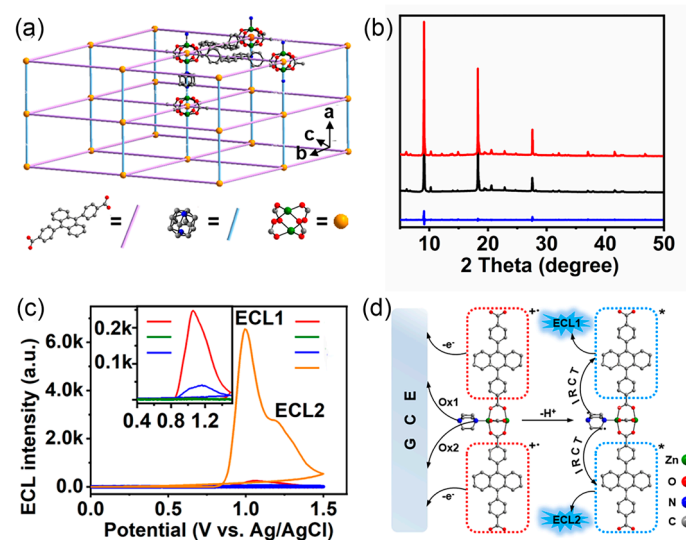


Figure 5. (a) Three-dimensional structure of m-MOF. (b) PXRD pattern of m-MOF (black), simulated result (red), and their difference (blue). (c) ECL curves of DPA-modified GCEs (red) in presence of DABCO, and of DPA-(green), s-MOF-(blue), and m-MOF (orange)-modified GCEs in 0.1 M PBS. (d) Stepwise ECL mechanism of m-MOF. “*” represents the excited state. Reproduced from [66] with permission from American Chemical Society.

As a novel member of frameworks, COFs gradually became fascinating in ECL applications. Firstly, Li et al. gave general advice on how to design COFs with highly efficient ECL [67]. Meanwhile, Lei's group provided a detailed mechanism on the enhanced ECL of COFs [68]. Based on donor–acceptor (D-A) units, a luminescent *t*-COF was synthesized as an ECL emitter by integrating triazine and triphenylamine as donor and acceptor units in the reticular skeleton, respectively (Figure 6a). Revealed with a PXRD analysis, the *t*-COF showed a crystalline structure with diffraction peaks at $2\theta = 4.4, 7.7, 8.9, 11.8,$ and 22.5° , which were assigned to the 100, 110, 200, 210, and 001 facets, respectively (Figure 6b). Compared to the other two COFs, *t*-COF had a magnificent ECL performance in TPrA/PBS (Figure 6c), indicating the importance of a D-A structure in *t*-COF during an ECL reaction. The simulated charge density difference between the first excited state and ground state of COF demonstrated an electron density loss on the triazine units and an electron density gain on the triphenylamine units, confirming the charge transfer between triphenylamine and triazine units (Figure 6d). Furthermore, the efficient charge transfer could be identified with the movement of HOS/LUS to the Fermi level when holes/electrons were doped (Figure 6e). Finally, the competitive oxidation mechanism involved the triazine unit gaining electrons from TPrA \cdot^+ while the triphenylamine unit was oxidized by oxidative TPrA $^{+\bullet}$ (Figure 6f, left) or the electrode (Figure 6f, right), leading to dual ECL emissions.

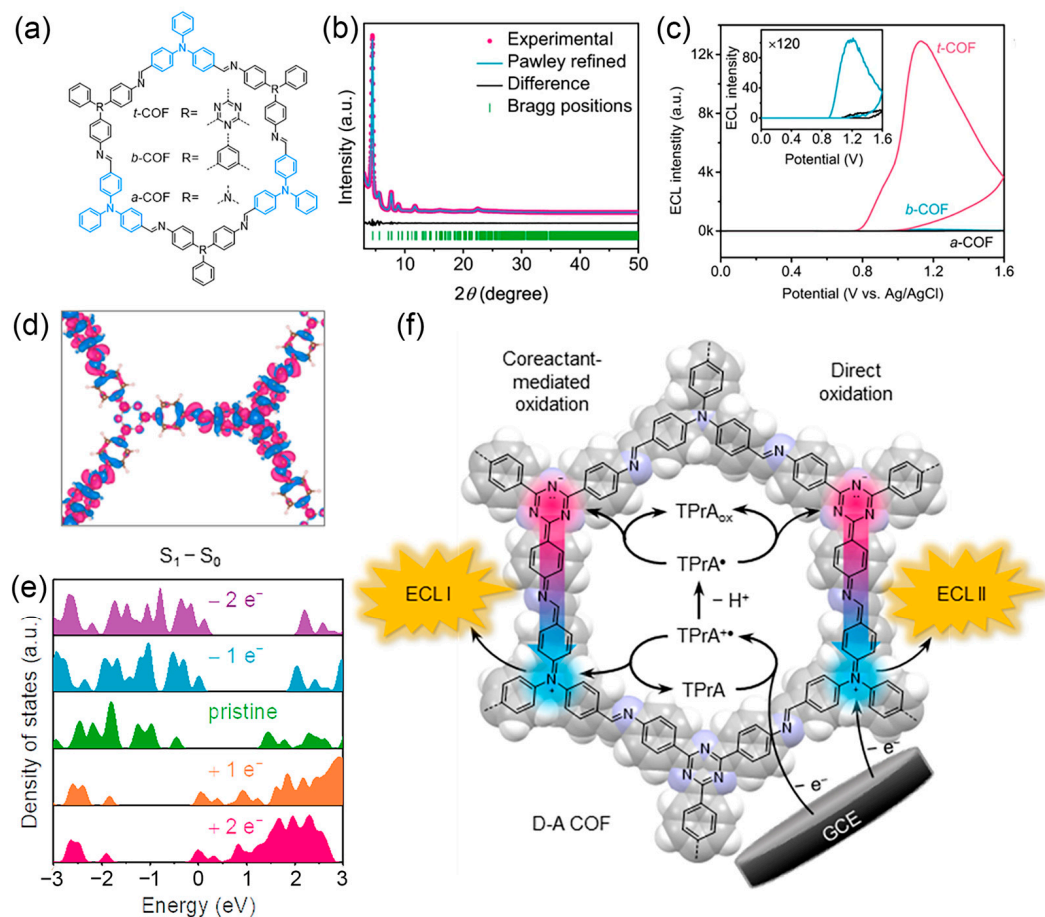


Figure 6. (a) Structure of TFPA-based COFs. (b) PXRD patterns of *t*-COF and their difference. (c) ECL curves of three COF-modified GCEs in the presence of 20 mM of TPrA. (d) The difference in charge density between the first excited state and ground state of *t*-COF. (e) Density of states of *t*-COF doped with different electron/hole numbers. (f) Competitive oxidation mechanism via intrareticular charge transfer. Reproduced from [68] with permission from the Nature Publishing Group.

HOFs comprised solely of pure organic or metal–organic units connected by intermolecular H-bonds were also found to have ECL enhancement properties compared to

their monomers. Zhang et al. synthesized a triazinyl-based HOF through N···H hydrogen bond self-assembly aggregation. The resulting HOF showed a highly enhanced ECL efficiency (21.3%) relative to the Ru(bpy)₃²⁺ standard, and was applied for ultrasensitive kanamycin biosensing [69]. Benefiting from the densely stacked structure, Lei's group proposed the HOF-based ECL enhancement mechanism via the intrareticular electron coupling (IREC) pathway [70]. Utilizing multiple H-bonds and π -interactions, HOF-101 with 1,3,6,8-tetra(4-carboxylphenyl)pyrene as a ligand was synthesized (Figure 7a). Compared with 1,3,6,8-tetracarboxypyrene-based HOF-100 and a bare electrode, HOF-101 modified GCE showed significantly enhanced ECL in the presence of TPrA due to the IREC effect (Figure 7b). Through model simulation, the charge density difference between S₁ and S₀ of HOF-101 was illustrated (Figure 7c), showing a mutual electron density depletion and accumulation of vertical stacking units. This IREC pathway in HOF-101 achieves ECL enhancement by accelerating electron transfer between anion radicals and cation radicals (Figure 7d).

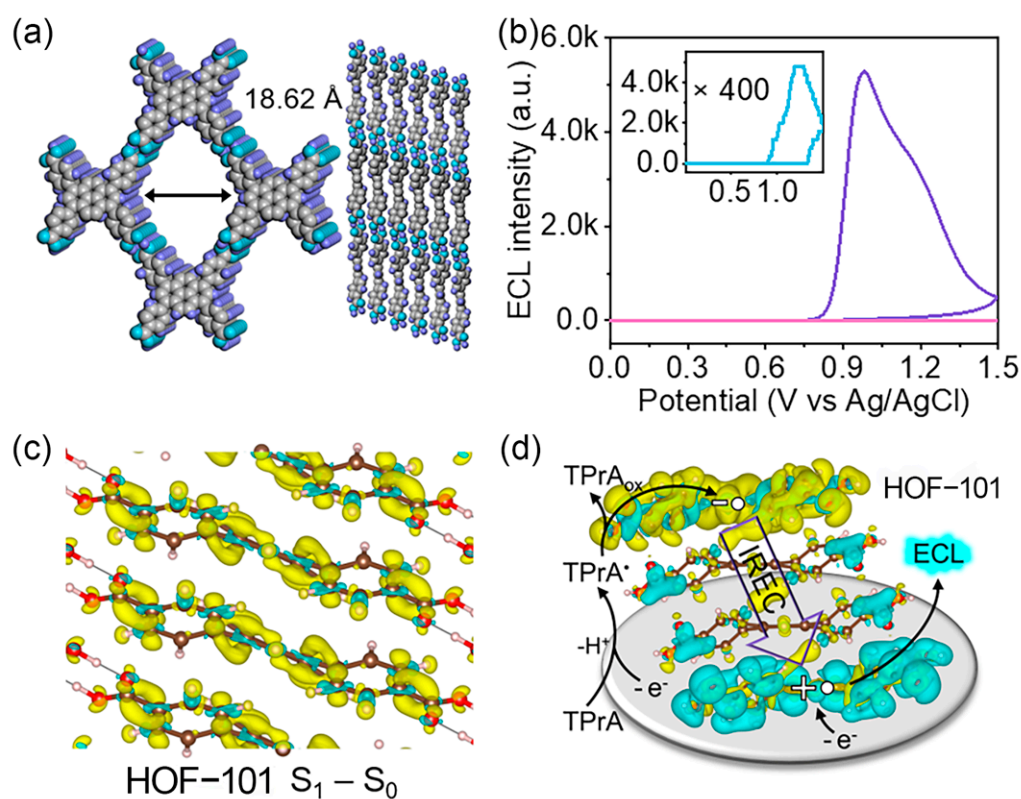


Figure 7. (a) Pore structure and stacking of HOF-101. (b) ECL curves of HOF-101 (purple), HOF-100 (blue), and a bare electrode (pink) in the presence of 20 mM of TPrA. (c) The difference of charge density distribution between S₁ and S₀ of HOF-101. (d) IREC-driven ECL mechanism of HOF-101 with a neutral charge density difference. Reproduced from [70] with permission from the Royal Society of Chemistry.

3. Framework-Enhanced ECL for Biosensing

The sensitive, specific, and reliable detection of tumor markers is vital for the early diagnosis of cancer, which brings hope to human patients for cancer prevention. Based on unique physical properties, chemical compositions, and functional methods, framework-enhanced ECL may provide an ultrasensitive and comprehensive assay for monitoring these markers. By combining with biological tools, framework-based biosensors can distinguish various biomarkers such as proteins, nucleic acid, cells, and small molecules in a clinical analysis.

3.1. Proteins

Proteins are typical biomacromolecules that are generally analyzed through immunoassays. Once a protein is clinically certified as a disease-related biomarker for a diagnosis, it will receive much attention in ultrasensitive detection. For example, to improve the survival of patients, cancer markers are of great significance in the guidance of an early tumor diagnosis and introducing appropriate targeted therapies [71]. Integrating with highly specific immunoreactions, ECL immunoassays are powerful tools for protein detections. Alpha-fetoprotein (AFP) is a well-known biomarker for the diagnosis of a liver malignant tumor [72]. Zhao et al. synthesized bimetallic NiZn MOF nanosheets to amplify cathodic luminol ECL through the synergistic effect of the bimetallic catalyst in AFP immunodetection [73]. Li et al. designed a signal-off ECL biosensor for AFP detection by utilizing the MnO₂ nanosheet/polydopamine dual-quenching effect towards a Ru(bpy)₃²⁺-functionalized MOF [74].

Cytokeratin 19 fragment 21–1 is recognized as an essential biomarker of non-small-cell lung cancer with a high specificity. Wei's group constructed a "signal-on" ECL immunosensor for this biomarker detection by using a copper-doped terbium MOF as a luminescent tag, which exhibited a strong ECL emission with K₂S₂O₈ as a coreactant through electrocatalyzing the reduction of S₂O₈²⁻ [75]. In the same group, a biocompatible tris(4,4'-dicarboxylic acid-2,2'-bipyridyl)ruthenium(II) [Ru(dcbpy)₃²⁺]-functionalized γ -cyclodextrin MOF not only served as a carrier to immobilize the detection antibody via a Pd-N bond but also facilitated the electron transfer rate to amplify the ECL signal [76], providing the ultrasensitive method for an early diagnosis of lung cancer.

Through potential-resolved ECL, a reticular biosensor could detect multiple protein biomarkers in a single run. Zhang et al. developed a MOF-based ECL tag with both anodic and cathodic emission [77]. A useful strategy with the isolated anodic and cathodic coreactants was applied to improve the analytical performance of this potential-resolved ECL sensor, leading to a successful analysis of a carcinoembryonic antigen (CEA) and neuron-specific enolase (NSE) simultaneously.

According to the different roles of frameworks in ECL processes, various signal transductions can be realized in an analysis of the same targets. For example, a hollow hierarchical MOF was employed as a carrier to graft Ru complexes as a signal amplification with the catalytic hairpin assembly strategy [78], showing an excellent selectivity and high sensitivity for thrombin determination. By tuning the reaction time, a series of porphyrin Zr-MOFs (PCN-222) with different specific surface areas, pore sizes, structures, and surface charge states were synthesized (Figure 8a), which served as an ECL emitter, coreactant promoter, and connection in the ECL immunoassay [79]. Furthermore, Xiao's group designed a COF-based ECL biosensor with conductivity- and pre-reduction-enhanced ECL, which overcame the intrinsic poor conductivity of COF [80]. With the aid of the signal amplification of the aptamer/protein-proximity-binding-induced 3D bipedal DNA walker, the constructed ECL sensor realized the supersensitive detection of thrombin (Figure 8b).

In addition, some proteins can be detected by utilizing their bioactive properties. For example, telomerase can extend the length of specific DNA, indicating its possible role as a signal switch. By monitoring bioactivity, telomerase was already analyzed with several well-designed ECL methods [81,82]. In Lei's group, an ECL telomerase biosensor was proposed with a BODIPY-based MOF nanoemitter composed of pyridine-substituted BODIPY, a terephthalic acid ligand, and Zn nodes (Figure 9a) [83]. The BODIPY-based MOF showed the P6/m trigonal crystal system, reducing the over-aggregation of BODIPY for enhanced optical signals (Figure 9b). After an elaborative design, the BODIPY-based MOF ECL sensors reached a good sensitivity under different telomerase concentrations (Figure 9c). The mechanism of this sensor was that the DNA hairpin opened when telomerase appeared, allowing the MOF to approach the electrode surface for ECL signal generation (Figure 9d). Integrating with unique immunoreactions, framework-based ECL biosensors become powerful for protein detection (Table 1).

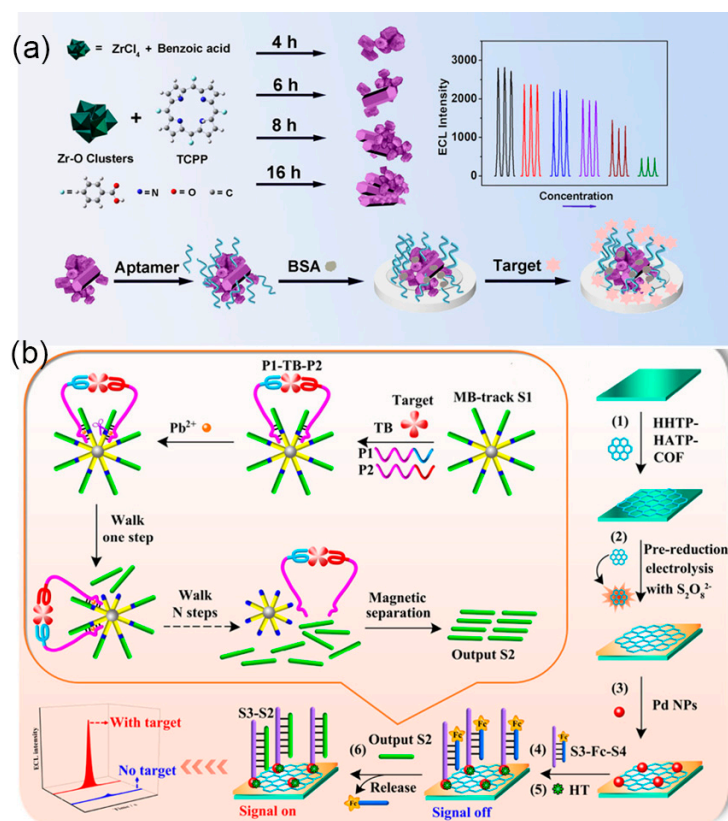


Figure 8. (a) Stepwise construction of PCN-222-based thrombin biosensor. Reproduced from [79] with permission from American Chemical Society. (b) Preparation procedure and DNA walker amplification principle of COF-based ECL sensor. Reproduced from [80] with permission from American Chemical Society.

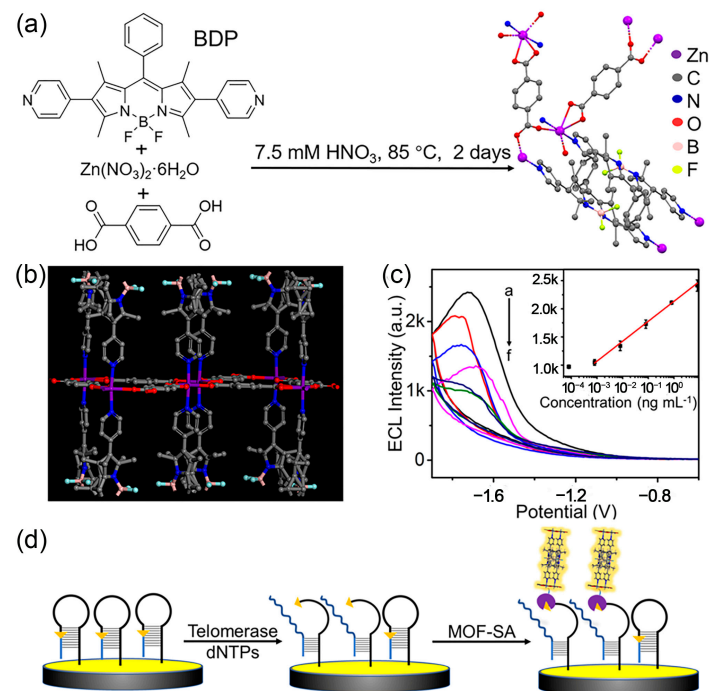


Figure 9. (a) Synthesis of the BODIPY-based MOF. (b) The spatial structure of MOFs. (c) ECL response under different telomerase concentrations. (d) Schematic diagram of the stepwise telomerase recognition. Reproduced from [83] with permission from the Royal Society of Chemistry.

Table 1. A summary of framework-enhanced ECL for detection of proteins.

Targets	Frameworks	Linear Range	LOD	Ref.
AFP	NiZn MOF	0.00005 to 100 ng/mL	0.98 fg/mL	[73]
AFP	Ru(bpy) ₃ ²⁺ @TMU-3	0.01 pg/mL to 5 ng/mL	10.7 fg/mL	[74]
AFP	Magnetic MOF@CdSnS	1 fg/mL to 100 ng/mL	0.2 fg/mL	[84]
CYFRA21-1	Pd-ZIF-67	0.01 to 100 ng/mL	2.6 pg/mL	[75]
CYFRA21-1	Ru@ γ -CD-MOF	0.1 pg/mL to 50 ng/mL	0.048 pg/mL	[76]
Thrombin	Ru-UiO-66-NH ₂	100 fM–100 nM	31.6 fM	[78]
Thrombin	PCN-222	50 fg/mL to 100 pg/mL	2.48 fg/mL	[79]
Thrombin	Conductive COF	100 aM to 1 nM	62.1 aM	[80]
Telomerase	BODIPY MOF	8.0×10^{-4} to 8.0 ng/mL	0.43 pg/mL	[83]
PSA	Ru-MOF	5 pg/mL to 5 μ g/mL	1.78 pg/mL	[85]
PSA	MOF/Au/DNAzyme	0.5 to 500 ng/mL	0.058 ng/mL	[86]
CEA	N,B-doped Eu MOF	0.1 pg/mL to 1 μ g/mL	0.06 pg/mL	[87]
NSE	J-aggregated MOF	10 pg/mL to 50 ng/mL	7.4 pg/mL	[88]
Peptide	Cu:Tb-MOF	1.0 pg/mL to 50 ng/mL	0.68 pg/mL	[89]
ALP	π -conjugated COF	0.01 to 100 U/L	7.6×10^{-3} U/L	[90]
D-dimer	RuZn MOFs	0.001–200 ng/mL	0.20 pg/mL	[91]

3.2. Nucleic Acids

In the analysis of nucleic acids, signal amplification techniques such as a catalytic hairpin assembly (CHA) [92], rolling circle amplification [93], and hybridization chain reaction [94] have been widely used for a long time. The Crispr/Cas12a technique is also utilized for an enhanced ECL signal in DNA biosensing [95]. Combined with these powerful tools, a series of framework-based ECL genosensors are being developed rapidly for ultrasensitive nucleic acid detection.

As noncoding RNAs, microRNAs (miRNAs) regulate the expression of messenger RNA by binding to complementary sequences. Once alterations in miRNA expression happen, messenger RNA expression is disrupted, which leads to potential oncogenic changes [96]. Therefore, it is crucial to construct reliable and sensitive biosensors for miRNA detection. With the structural development of frameworks, framework-based ECL genosensors for a miRNA analysis were extensively investigated. For instance, Wang et al. synthesized a Zn MOF as a self-enhanced ECL emitter with dual ligands of DPA and *N,N*-diethylethylenediamine for miRNA-21 detection [97]. DPA is a typical luminophore in ECL while DEAEA could be used as both a coreactant and a morphologic regulator, which leads to a strong and stable ECL emission with the efficient intramolecular electron transfer process. Based on CHA and ECL resonance energy transfer, this sensor realized ‘signal-off’-mode signal amplification in the presence of miRNA-21. Similarly, Xue et al. developed a microRNA-141 ECL bioassay by using a dual-ligand MOF, which simultaneously contained a luminophore TPE derivative and a coreactant ligand (1,4-diazabicyclo[2.2.2]octane) in the structural unit [98]. Using a DNA triangular prism as a signal switch to detect microRNA-141, this ECL biosensor achieved a low detection limit at the level of 22.9 aM. Furthermore, a dual-wavelength multifunctional ECL biosensor was established for the rapid simultaneous detection of dual targets miRNA-141 and miRNA-155 [99]. As shown in Figure 10a, a Zr MOFs@PEI@AuAg nanocomposite exhibited intense and stable dual-wavelength ECL emissions. Since ECL emissions of the nanocomposite at two wavelengths of 535 nm and 644 nm were both quenched by resonance energy transfer, this sensor achieved a good linear relation for the miRNA analysis at two different wavelengths (Figure 10b). The experiment of ECL stability showed a low signal change, indicating a good accuracy and convincing stability in the simultaneous detection of miRNAs (Figure 10c). In addition, the classic-DNA-walker-based signal amplification strategy is also used for a MOF sheet-based ECL sensor in the detection of oral cancer overexpressed 1 gene [100].

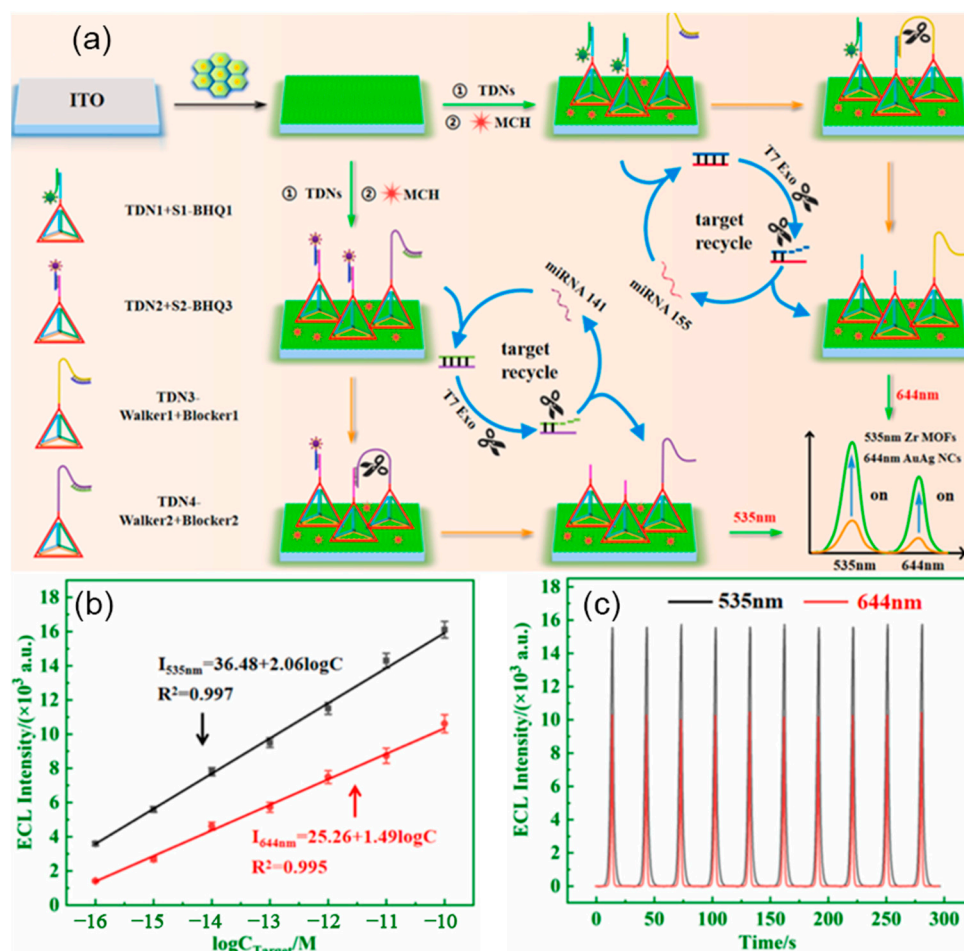


Figure 10. (a) Schematic illustration of ECL biosensing platform based on Zr MOFs@PEI@AuAg nanocomposite for simultaneous detection of dual microRNAs. (b) Plot of the ECL intensity as a function of the logarithm of target miRNAs' concentration at 535 nm and 644 nm. (c) ECL signal stability. Reproduced from [99] with permission from Elsevier.

To overcome an intrinsic low conductivity in MOFs, a conductive NiCo bimetal-organic framework nanorod was successfully applied in miRNA-141 detection, broadening the horizon of conductive MOFs in ECL sensing applications [101]. Furthermore, with the long-range orderly arrangement and effective intramolecular charge transfer, a pyrene-based sp^2 COF was synthesized as an efficient ECL emitter via the polycondensation of tetrakis(4-formylphenyl)pyrene and 2,2'-(1,4-phenylene)-diacetonitrile. Because of topologically linking pyrene luminophores and aggregation-induced emissive luminogens, the luminescent COF showed a strong and stable ECL emission [102], leading to a highly sensitive microRNA-21 biosensor.

As a great threat to health, viruses also receive much attention in ultrasensitive detection. For instance, the Zika virus, a member of the Flaviviridae virus family, is suspected to be associated with severe congenital malformations [103]. Mao's group quantified the Zika virus based on Zr-based metal-organic gel and Fe-MIL-88 MOFs as an electrode matrix and nanotag, respectively [104]. The double quenching effect originated from Fe-MIL-88 MOFs as both an ECL acceptor and metal active centers to consume the coreactant, resulting in a distinct turn-off signal in the presence of the virus. On the other hand, Shan's group designed a 2D MOF with an excellent ECL performance by combining the photosensitizer ZnTCPP and electroactive $[\text{Co}_2(-\text{CO}_2)_4]$ secondary building units for a Sars-CoV-2 gene analysis [105]. The ECL sensor achieved a rapid nonamplified detection of the RdRp gene of SARS-CoV-2 with an extremely low limit of detection (30 aM). Furthermore, Wu et al. designed an ECL biosensor using PCN-224/ZnO/polyacrylamide as signal tag for an accu-

rate analysis of the HPV-16 virus [106]. With the aid of multiple target-cycling amplification technologies and HCR reactions, this method achieved a rapid and effective “signal-off” detection of the target with the detection limit of 0.13 fM.

Overall, by integrating appropriate frameworks with well-designed DNA sequences, these above methods show a great performance in a nucleic acid analysis, which expands the application of frameworks in biosensing.

3.3. Small Molecules

Compared to traditional analytical methods like chromatography and enzyme catalysis, framework-based ECL methods are more sensitive and convenient for small molecule detection. For the determination of small molecules, utilizing specific recognition between an aptamer and target is the most common strategy. For instance, the transduction of aptamer configurations alters the distance between a signal promoter and ECL luminophores, resulting in a signal change by introducing target molecules (Figure 11a). A plasmon-enhanced ECL aptasensor displayed highly sensitive detection for lincomycin [107]. Based on a suitable aptasensor, a wide range of molecules can be efficiently detected, such as kanamycin [108], sulfadimethoxine [109], and isocarboxiphos [110]. Apart from the aptamer, a competition-type ECL immunosensor using Pt NPs@MOFs for the quantitative detection of trenbolone was successfully constructed, demonstrating the simplicity of framework-based ECL systems [111].

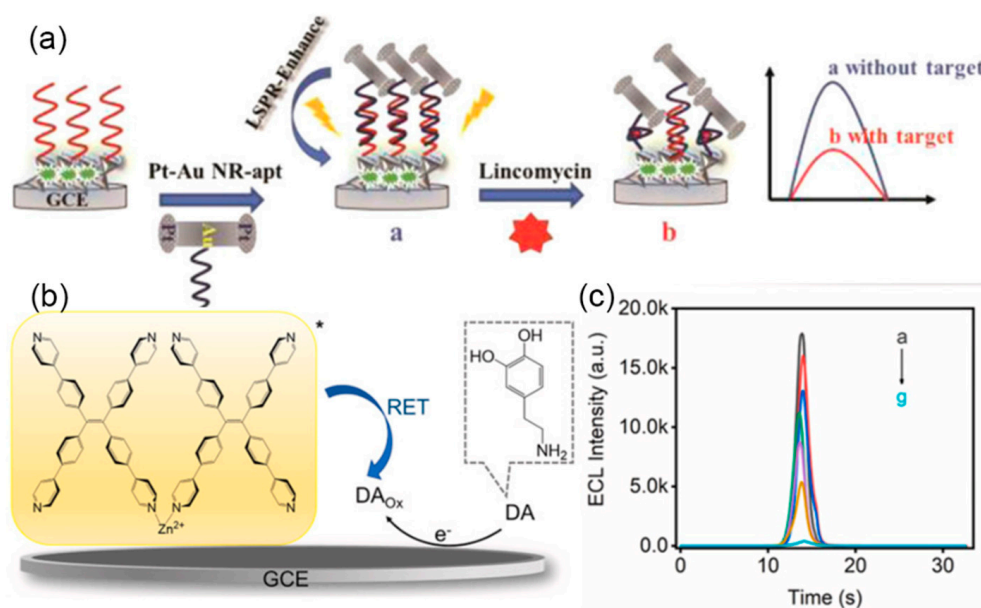


Figure 11. (a) Stepwise illustration of Eu MOF-based aptasensor for lincomycin detection. Reproduced from [107] with permission from American Chemical Society. (b) Quenching mechanism of dopamine ECL detection. (c) Variation of ECL intensity at different concentrations of dopamine: 0, 0.01, 0.1, 1, 10, 100, and 1000 μM from (a) to (g). Reproduced from [55] with permission from Elsevier.

Based on the quenching effect between MOF radicals and oxidized dopamine (Figure 11b), dopamine can be analyzed without the aid of an aptamer [55]. This hindrance to ECL was highly relevant to the dopamine concentration, and then was applied to construct an ECL method for the highly sensitive detection of dopamine in serum samples (Figure 11c). Similarly, uric acid [112], rutin [113], and deoxynivalenol [114] can also be directly measured with framework-based ECL sensors. In addition, a MOF/COF-mixed emitter with dual-color ECL was prepared [115]. Based on a π - π interaction between targets and a MOF/COF, diclazepam can not only be absorbed but also selectively quench ECL, achieving sensitive detection.

Furthermore, metal ions with potential harm to human health are generally analyzed with inductively coupled plasma mass spectrometry, ion chromatography, and atomic

absorption spectroscopy, requiring expensive instruments and staff costs. The inhibition effect of metal ions towards ECL makes them detectable through well-designed framework-based ECL sensors [116].

3.4. Cellular Analysis

ECL-based cellular analyses [117], such as circulating tumor cells (CTCs) [118] and the cell matrix [119], have been developed for several decades. With the combination of ECL biotechnology, framework-based ECL sensors for a cell-related analysis gradually emerge. In a typical manner, Liu's group realized single-molecule movement visualization at the cellular membrane through capturing photoluminescence signals of the designed Ru(bpy)₃²⁺-embedded MOF complex (RuMOF) [120]. With the aid of the nanoconfinement effect within frameworks, RuMOFs had a splendid ECL intensity at the single-molecule level, which was conducive to visualize the distribution of RuMOF-labeled-membrane PTK7 proteins at low-expressing cells, demonstrating a great potential of framework-based ECL systems in cellular monitoring.

Bacteria may cause great harm to health while existing in the human circulatory system, indicating the importance of sensitive detection. Utilizing steric hindrance on electron transfer, *Vibrio parahaemolyticus* [121] and *Escherichia coli* [122] can be successfully analyzed with ECL sensors based on Ru-MOF and NH₂-MIL-53(Al) signal reporters, respectively. In addition, an exosome as a subcellular structure is also accurately detected using well-designed ECL sensors with a different signal transduction. For example, Cui's group constructed a label-free HepG₂-derived exosome ECL sensor based on the selectivity of the CD63 peptide in recognizing CD63 proteins on the exosome surface and strong coordination interactions between the Zr⁴⁺ of Zn-TCPP/UiO-66-NH₂ and the phosphate head of exosomes (Figure 12). The ECL biosensor exhibited a good sensitivity with a detection range from 1.00 × 10⁴ to 3.16 × 10⁶ particles/μL, which is better than most of the existing label-free methods for detecting exosomes [123], showing the great prospects of framework-based ECL in sensitive bioassays.

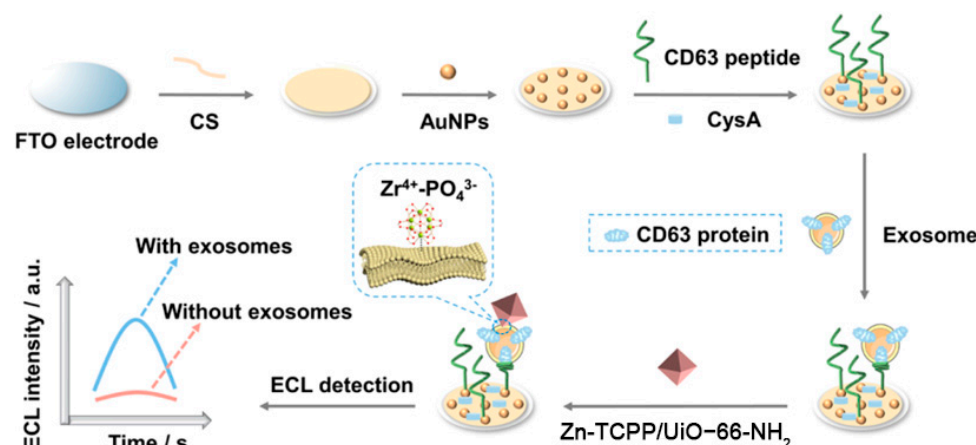


Figure 12. ECL biosensor construction and detecting HepG₂-derived exosomes. Reproduced from [123] with permission from American Chemical Society.

4. Conclusions and Perspectives

Frameworks are a kind of widely used material in an ECL analysis owing to the flexible structure, long-range ordered units, and controllable modification with some recognition elements. According to the functions in the ECL process, frameworks have been exploited as a carrier of luminophores, a catalyst of ECL reactions, and crystalline emitters. Based on the innovation of ECL mechanisms, reticular biosensors gain a more efficient ECL for signal amplification, which improves the sensitivity of biosensing. Different from MOFs, metal-free COFs and HOFs have been rapidly developed and constructed lots of biocompatible analytical methods. To date, framework-based ECL biosensors have been successfully

utilized in the detection of proteins, nucleic acids, small molecules, and cells by integrating specific functional materials, facilitating the further development of ECL techniques.

Actually, the research on framework-based ECL systems is much more mature than several years ago but challenges still exist. To further expand their application and improve their biosensing performance, some aspects should be deliberated in future works. (1) It is crucial to explore near-infrared ECL-active frameworks for developing in vivo biosensing and bioimaging because of a good penetrability and low scattering in NIR [124]. (2) The 3D-sp²-carbon-conjugated COFs may accelerate charge transfer through the largely conjugated electron structure, resulting in a high ECL efficiency. (3) In order to develop a single-molecule ECL imaging technique [125], frameworks at the nanoscale with an intense ECL emission are promising crystalline nanoemitters. (4) The framework characteristics of self-luminescence such as the orthogonal luminescence lifetime [126] can be endowed through the introduction of lanthanide elements, which may be used for designing ECL sensors. (5) Multivariate MOFs containing multiple metals have a greater selectivity in catalysis for the acceleration of charge transfer, which improves the efficiency of ECL reactions, leading to a strong ECL emission [127]. (6) New types of methods for reticular nanoemitter construction should be discovered, which may simplify synthesis. (7) The conductivity of framework-based emitters should be improved by integrating the redox-active ligands in the frameworks [128]. In a word, the key of ECL techniques relies heavily on the improvement of emitters, suggesting that ECL-active frameworks with a good stability, easy accessibility, and high ECL efficiency are urgently required in future research.

Author Contributions: Conceptualization, H.F. and J.L.; writing—original draft preparation, writing—review and editing, H.F., Z.X., H.H., R.L., H.J. and J.L.; visualization, H.F. and J.L.; funding acquisition, H.J. and J.L. All authors have read and agreed to the published version of the manuscript.

Funding: This research was supported by the National Natural Science Foundation of China (22274071, 22234005, 21890741), the Natural Science Foundation of Jiangsu Province (BZ2021010), the Fundamental Research Funds for the Central Universities (020514380297), and the State Key Laboratory of Analytical Chemistry for Life Science (5431ZZXM2204).

Institutional Review Board Statement: Not applicable.

Informed Consent Statement: Not applicable.

Data Availability Statement: Not applicable.

Conflicts of Interest: The authors declare no conflict of interest.

References

1. Miao, W. Electrogenated chemiluminescence and its biorelated applications. *Chem. Rev.* **2008**, *108*, 2506–2553. [[CrossRef](#)] [[PubMed](#)]
2. Richter, M.M. Electrochemiluminescence (ECL). *Chem. Rev.* **2004**, *104*, 3003–3036. [[CrossRef](#)] [[PubMed](#)]
3. Wu, P.; Hou, X.; Xu, J.; Chen, H. Electrochemically generated versus photoexcited luminescence from semiconductor nanomaterials: Bridging the valley between two worlds. *Chem. Rev.* **2014**, *114*, 11027–11059. [[CrossRef](#)] [[PubMed](#)]
4. Chen, S.; Lei, Y.; Xu, J.; Yang, Y.; Dong, Y.; Li, Y.; Yi, H.; Liao, Y.; Chen, L.; Xiao, Y. Simple, rapid, and visual electrochemiluminescence sensor for on-site catechol analysis. *RSC Adv.* **2022**, *12*, 17330–17336. [[CrossRef](#)] [[PubMed](#)]
5. Wang, N.; Gao, H.; Li, Y.; Li, G.; Chen, W.; Jin, Z.; Lei, J.; Wei, Q.; Ju, H. Dual intramolecular electron transfer for in situ coreactant embedded electrochemiluminescence microimaging of membrane protein. *Angew. Chem. Int. Ed.* **2021**, *60*, 197–201. [[CrossRef](#)]
6. Dong, J.; Lu, Y.; Xu, Y.; Chen, F.; Yang, J.; Chen, Y.; Feng, J. Direct imaging of single-molecule electrochemical reactions in solution. *Nature* **2021**, *596*, 244–249. [[CrossRef](#)]
7. You, F.; Wei, Z.; Yuan, R.; Qian, J.; Long, L.; Wang, K. Sensitive and stable detection of deoxynivalenol based on electrochemiluminescence aptasensor enhanced by 0D/2D homojunction effect in food analysis. *Food Chem.* **2023**, *403*, 134397. [[CrossRef](#)]
8. Wang, C.; Pei, Y.; Liu, P.; Li, Y.; Wang, Z. Donor-acceptor structure-dependent electrochemiluminescence sensor for accurate uranium detection in drinking water. *ACS Sustain. Chem. Eng.* **2022**, *10*, 14665–14670. [[CrossRef](#)]
9. Chen, M.-M.; Xu, C.-H.; Zhao, W.; Chen, H.-Y.; Xu, J.-J. Single cell imaging of electrochemiluminescence-driven photodynamic therapy. *Angew. Chem. Int. Ed.* **2022**, *61*, e202117401.
10. Shen, Y.; Tian, Q.; Sun, Y.; Xu, J.-J.; Ye, D.; Chen, H.-Y. ATP-activatable photosensitizer enables dual fluorescence imaging and targeted photodynamic therapy of tumor. *Anal. Chem.* **2017**, *89*, 13610–13617. [[CrossRef](#)]

11. Yang, Y.; Hou, W.; Liu, S.; Sun, K.; Li, M.; Wu, C. Biodegradable polymer nanoparticles for photodynamic therapy by bioluminescence resonance energy transfer. *Biomacromolecules* **2018**, *19*, 201–208. [[CrossRef](#)] [[PubMed](#)]
12. Yin, B.; Ho, W.K.H.; Xia, X.; Chan, C.K.W.; Zhang, Q.; Ng, Y.M.; Lam, C.Y.K.; Cheung, J.C.W.; Wang, J.; Yang, M.; et al. A multilayered mesoporous gold nanoarchitecture for ultraeffective near-infrared light-controlled chemo photothermal therapy for cancer guided by SERS imaging. *Small* **2023**, *19*, 2206762. [[CrossRef](#)] [[PubMed](#)]
13. Wei, X.; Zhu, M.; Yan, H.; Lu, C.; Xu, J. Recent advances in aggregation-induced electrochemiluminescence. *Chem. Eur. J.* **2019**, *25*, 12671–12683. [[CrossRef](#)]
14. Wang, T.; Wang, D.; Padelford, J.W.; Jiang, J.; Wang, G. Near-infrared electrogenerated chemiluminescence from aqueous soluble lipoic acid Au nanoclusters. *J. Am. Chem. Soc.* **2016**, *138*, 6380–6383. [[CrossRef](#)]
15. Stewart, A.J.; Brown, K.; Dennany, L. Cathodic quantum dot facilitated electrochemiluminescent detection in blood. *Anal. Chem.* **2018**, *90*, 12944–12950. [[CrossRef](#)] [[PubMed](#)]
16. Jin, Z.; Zhu, X.; Wang, N.; Li, Y.; Ju, H.; Lei, J. Electroactive metal-organic frameworks as emitters for self-enhanced electrochemiluminescence in aqueous medium. *Angew. Chem. Int. Ed.* **2020**, *59*, 10446–10450. [[CrossRef](#)]
17. Furukawa, H.; Cordova, K.E.; O’Keeffe, M.; Yaghi, O.M. The chemistry and applications of metal-organic frameworks. *Science* **2013**, *341*, 1230444. [[CrossRef](#)]
18. Geng, K.; He, T.; Liu, R.; Dalapati, S.; Tan, K.T.; Li, Z.; Tao, S.; Gong, Y.; Jiang, Q.; Jiang, D. Covalent organic frameworks: Design, synthesis, and functions. *Chem. Rev.* **2020**, *120*, 8814–8933.
19. Cai, G.; Yan, P.; Zhang, L.; Zhou, H.; Jiang, H. Metal-organic framework-based hierarchically porous materials: Synthesis and applications. *Chem. Rev.* **2021**, *121*, 12278–12326. [[CrossRef](#)] [[PubMed](#)]
20. Lyu, S.; Guo, C.; Wang, J.; Li, Z.; Yang, B.; Lei, C.; Wang, L.; Xiao, J.; Zhang, T.; Hou, Y. Exceptional catalytic activity of oxygen evolution reaction via two-dimensional graphene multilayer confined metal-organic frameworks. *Nat. Commun.* **2022**, *13*, 6171. [[CrossRef](#)] [[PubMed](#)]
21. Xu, Y.; Yin, X.B.; He, X.W.; Zhang, Y.K. Electrochemistry and electrochemiluminescence from a redox-active metal-organic framework. *Biosens. Bioelectron.* **2015**, *68*, 197–203. [[CrossRef](#)]
22. Liao, X.; Fu, H.; Yan, T.; Lei, J. Electroactive metal-organic framework composites: Design and biosensing application. *Biosens. Bioelectron.* **2019**, *146*, 111743. [[CrossRef](#)] [[PubMed](#)]
23. Han, Z.; Wang, J.; Du, P.; Chen, J.; Huo, S.; Guo, H.; Lu, X. Highly facile strategy for detecting D₂O in H₂O by porphyrin-based luminescent probes. *Anal. Chem.* **2022**, *94*, 8426–8432. [[CrossRef](#)] [[PubMed](#)]
24. Zhang, Y.-J.; Yang, Y.; Wang, J.-M.; Liang, W.-B.; Yuan, R.; Xiao, D.-R. Electrochemiluminescence enhanced by isolating ACQphores in pyrene-based porous organic polymer: A novel ECL emitter for the construction of biosensing platform. *Anal. Chim. Acta* **2022**, *1206*, 339648. [[CrossRef](#)] [[PubMed](#)]
25. Zhang, B.; Kong, Y.; Liu, H.; Chen, B.; Zhao, B.; Luo, Y.; Chen, L.; Zhang, Y.; Han, D.; Zhao, Z.; et al. Aggregation-induced delayed fluorescence luminogens: The innovation of purely organic emitters for aqueous electrochemiluminescence. *Chem. Sci.* **2021**, *12*, 13283–13291. [[CrossRef](#)]
26. Bahari, D.; Babamiri, B.; Moradi, K.; Salimi, A.; Hallaj, R. Graphdiyne nanosheet as a novel sensing platform for self-enhanced electrochemiluminescence of MOF enriched ruthenium (II) in the presence of dual co-reactants for detection of tumor marker. *Biosens. Bioelectron.* **2022**, *195*, 113657. [[CrossRef](#)]
27. Dai, W.; Wang, X.; Chen, G.; Wang, X.; Hu, C.; Zhen, S.; Huang, C.; Li, Y. Facile synthesis of 2D Europium-metal organic frameworks nanosheets for highly efficient electrochemiluminescence in DNA detection. *Chem. Eng. J.* **2023**, *465*, 143037. [[CrossRef](#)]
28. Li, Y.-J.; Cui, W.-R.; Jiang, Q.-Q.; Liang, R.-P.; Li, X.-J.; Wu, Q.; Luo, Q.-X.; Liu, J.; Qiu, J.-D. Arousing electrochemiluminescence out of non-electroluminescent monomers within covalent organic frameworks. *ACS Appl. Mater. Interfaces* **2021**, *13*, 47921–47931. [[CrossRef](#)]
29. Cui, W.-R.; Li, Y.-J.; Jiang, Q.-Q.; Wu, Q.; Liang, R.-P.; Luo, Q.-X.; Zhang, L.; Liu, J.; Qiu, J.-D. Tunable covalent organic framework electrochemiluminescence from nonelectroluminescent monomers. *Cell Rep. Phys. Sci.* **2022**, *3*, 100630. [[CrossRef](#)]
30. Qin, X.; Zhao, X.; Wang, M.; Dong, Y.; Liu, J.; Zhu, Z.; Li, M.; Yang, D.; Shao, Y. Fabrication of tris(bipyridine)ruthenium(II)-functionalized metal-organic framework thin films by electrochemically assisted self-assembly technique for electrochemiluminescent immunoassay. *Anal. Chem.* **2018**, *90*, 11622–11628. [[CrossRef](#)] [[PubMed](#)]
31. Tang, T.; Yan, F.; Wang, L.; Zhao, C.; Nie, F.; Yang, G. A sandwich electrochemiluminescent assay for determination of concanavalin A with triple signal amplification based on MoS₂NF@MWCNTs modified electrode and Zn-MOF encapsulated luminol. *Microchim. Acta* **2020**, *187*, 523. [[CrossRef](#)] [[PubMed](#)]
32. Mo, G.; Qin, D.; Jiang, X.; Zheng, X.; Mo, W.; Deng, B. A sensitive electrochemiluminescence biosensor based on metal-organic framework and imprinted polymer for squamous cell carcinoma antigen detection. *Sens. Actuators B* **2020**, *310*, 127852. [[CrossRef](#)]
33. Qin, X.; Dong, Y.; Wang, M.; Zhu, Z.; Li, M.; Yang, Y.; Shao, Y. In situ growing triethanolamine-functionalized metal-organic frameworks on two-dimensional carbon nanosheets for electrochemiluminescent immunoassay. *ACS Sens.* **2019**, *4*, 2351–2357. [[CrossRef](#)] [[PubMed](#)]
34. Micheroni, D.; Lan, G.; Lin, W. Efficient electrocatalytic proton reduction with carbon nanotube-supported metal-organic frameworks. *J. Am. Chem. Soc.* **2018**, *140*, 15591–15595. [[CrossRef](#)]
35. Wang, S.; Zhao, Y.; Wang, M.; Li, H.; Saqib, M.; Ge, C.; Zhang, X.; Jin, Y. Enhancing luminol electrochemiluminescence by combined use of cobalt-based metal organic frameworks and silver nanoparticles and its application in ultrasensitive detection of cardiac troponin I. *Anal. Chem.* **2019**, *91*, 3048–3054. [[CrossRef](#)]

36. Feng, D.; Tan, X.; Wu, Y.; Ai, C.; Luo, Y.; Chen, Q.; Han, H. Electrochemiluminescence nanogears aptasensor based on MIL-53(Fe)@CdS for multiplexed detection of kanamycin and neomycin. *Biosens. Bioelectron.* **2019**, *129*, 100–106. [[CrossRef](#)]
37. Lu, Y.; Huang, X.; Wang, S.; Li, B.; Liu, B. Nanoconfinement-enhanced electrochemiluminescence for in situ imaging of single biomolecules. *ACS Nano* **2023**, *17*, 3809–3817. [[CrossRef](#)]
38. Diercks, C.S.; Liu, Y.; Cordova, K.E.; Yaghi, O.M. The role of reticular chemistry in the design of CO₂ reduction catalysts. *Nat. Mater.* **2018**, *17*, 301–307. [[CrossRef](#)]
39. Xue, X.; Gao, H.; Liu, J.; Yang, M.; Feng, J.; Liu, Z.; Lin, J.; Kasemchainan, J.; Wang, L.; Jia, Q.; et al. Electrostatic potential-derived charge: A universal OER performance descriptor for MOFs. *Chem. Sci.* **2022**, *13*, 13160–13171. [[CrossRef](#)]
40. Zhao, G.; Cai, C.; Cosnier, S.; Zeng, H.; Zhang, X.; Shan, D. Zirconium-metalloporphyrin frameworks as a three-in-one platform possessing oxygen nanocage, electron media, and bonding site for electrochemiluminescence protein kinase activity assay. *Nanoscale* **2016**, *8*, 11649–11657.
41. Yang, X.; Yu, Y.; Peng, L.; Lei, Y.; Chai, Y.; Yuan, R.; Zhuo, Y. Strong electrochemiluminescence from MOF accelerator enriched quantum dots for enhanced sensing of trace cTnI. *Anal. Chem.* **2018**, *90*, 3995–4002. [[CrossRef](#)] [[PubMed](#)]
42. Zhang, W.; Han, D.; Wu, Z.; Yang, K.; Sun, S.; Wen, J. Metal-organic layers-catalyzed amplification of electrochemiluminescence signal and its application for immunosensor construction. *Sens. Actuators B-Chem.* **2023**, *376*, 133004. [[CrossRef](#)]
43. Song, X.; Yu, S.; Zhao, L.; Guo, Y.; Ren, X.; Ma, H.; Wang, S.; Luo, C.; Li, Y.; Wei, Q. Efficient ABEI-dissolved O₂-Ce(III, IV)-MOF ternary electrochemiluminescent system combined with self-assembled microfluidic chips for bioanalysis. *Anal. Chem.* **2022**, *94*, 9363–9371. [[CrossRef](#)] [[PubMed](#)]
44. Zhou, J.; Li, Y.; Wang, W.; Tan, X.; Lu, Z.; Han, H. Metal-organic frameworks-based sensitive electrochemiluminescence biosensing. *Biosens. Bioelectron.* **2020**, *164*, 112332. [[CrossRef](#)] [[PubMed](#)]
45. Kent, C.A.; Mehl, B.P.; Ma, L.; Papanikolas, J.M.; Meyer, T.J.; Lin, W. Energy transfer dynamics in metal-organic frameworks. *J. Am. Chem. Soc.* **2010**, *132*, 12767–12769. [[CrossRef](#)] [[PubMed](#)]
46. Hou, C.; Li, T.; Cao, S.; Chen, Y.; Fu, W. Incorporation of a [Ru(dcbpy)(bpy)₂]²⁺ photosensitizer and a Pt(dcbpy)Cl₂ catalyst into metal-organic frameworks for photocatalytic hydrogen evolution from aqueous solution. *J. Mater. Chem. A* **2015**, *3*, 10386–10394. [[CrossRef](#)]
47. Yan, M.; Ye, J.; Zhu, Q.; Zhu, L.; Huang, J.; Yang, X. Ultrasensitive immunosensor for cardiac troponin I detection based on the electrochemiluminescence of 2D Ru-MOF nanosheets. *Anal. Chem.* **2019**, *91*, 10156–10163. [[CrossRef](#)]
48. Hu, G.; Xiong, C.; Liang, W.; Zeng, X.; Xu, H.; Yang, Y.; Yao, L.Y.; Yuan, R.; Xiao, D. Highly stable mesoporous luminescence-functionalized MOF with excellent electrochemiluminescence property for ultrasensitive immunosensor construction. *ACS Appl. Mater. Interfaces* **2018**, *10*, 15913–15919. [[CrossRef](#)]
49. Yang, Y.; Hu, G.; Liang, W.; Yao, L.; Huang, W.; Yuan, R.; Xiao, D. A highly sensitive self-enhanced aptasensor based on a stable ultrathin 2D metal-organic layer with outstanding electrochemiluminescence property. *Nanoscale* **2019**, *11*, 10056–10063. [[CrossRef](#)]
50. Zhou, Y.; He, J.; Zhang, C.; Li, J.; Fu, X.; Mao, W.; Li, W.; Yu, C. Novel Ce(III)-metal organic framework with a luminescent property to fabricate an electrochemiluminescence immunosensor. *ACS Appl. Mater. Interfaces* **2020**, *12*, 338–346. [[CrossRef](#)]
51. Wang, J.; Yao, L.; Huang, W.; Yang, Y.; Liang, W.; Yuan, R.; Xiao, D. Overcoming aggregation-induced quenching by metal-organic framework for electrochemiluminescence (ECL) enhancement: ZnPTC as a new ECL emitter for ultrasensitive MicroRNAs detection. *ACS Appl. Mater. Interfaces* **2021**, *13*, 44079–44085. [[CrossRef](#)]
52. Yao, L.; Yang, F.; Hu, G.; Yang, Y.; Huang, W.; Liang, W.; Yuan, R.; Xiao, D. Restriction of intramolecular motions (RIM) by metal-organic frameworks for electrochemiluminescence enhancement: 2D Zr₁₂-adb nanoplate as a novel ECL tag for the construction of biosensing platform. *Biosens. Bioelectron.* **2020**, *155*, 112099. [[CrossRef](#)]
53. Han, Z.; Zhang, Y.; Wu, Y.; Li, Z.; Bai, L.; Huo, S.; Lu, X. Substituent-induced aggregated state electrochemiluminescence of tetraphenylethene derivatives. *Anal. Chem.* **2019**, *91*, 8676–8682. [[CrossRef](#)]
54. Liu, J.; Zhang, J.; Tan, Z.; Zhuo, Y.; Chai, Y.; Yuan, R. Near-infrared aggregation-induced enhanced electrochemiluminescence from tetraphenylethylene nanocrystals: A new generation of ECL emitters. *Chem. Sci.* **2019**, *10*, 4497–4501. [[CrossRef](#)]
55. Fu, H.; Xu, Z.; Liu, T.; Lei, J. In situ coordination interactions between metal-organic framework nanoemitters and coreactants for enhanced electrochemiluminescence in biosensing. *Biosens. Bioelectron.* **2023**, *222*, 114920. [[CrossRef](#)] [[PubMed](#)]
56. Li, J.; Jia, H.; Ren, X.; Li, Y.; Liu, L.; Feng, R.; Ma, H.; Wei, Q. Dumbbell plate-shaped AIEgen-based luminescent MOF with high quantum yield as self-enhanced ECL tags: Mechanism insights and biosensing application. *Small* **2022**, *18*, 2106567. [[CrossRef](#)]
57. Yang, Y.; Hu, G.; Liang, W.; Yao, L.; Huang, W.; Zhang, Y.; Zhang, J.; Wang, J.; Yuan, R.; Xiao, D. An AIEgen-based 2D ultrathin metal-organic layer as an electrochemiluminescence platform for ultrasensitive biosensing of carcinoembryonic antigen. *Nanoscale* **2020**, *12*, 5932–5941. [[CrossRef](#)]
58. Kwok, R.T.K.; Leung, C.W.T.; Lam, J.W.Y.; Tang, B.Z. Biosensing by luminogens with aggregation-induced emission characteristics. *Chem. Soc. Rev.* **2015**, *44*, 4228–4238. [[CrossRef](#)]
59. Carrara, S.; Aliprandi, A.; Hogan, C.F.; De Cola, L. Aggregation-induced electrochemiluminescence of platinum(II) complexes. *J. Am. Chem. Soc.* **2017**, *139*, 14605–14610. [[CrossRef](#)]
60. Song, L.; Gao, W.; Han, Q.; Huang, Y.; Cui, L.; Zhang, C.-Y. Construction of an aggregation-induced electrochemiluminescent sensor based on an aminal-linked covalent organic framework for sensitive detection of glutathione in human serum. *Chem. Commun.* **2022**, *58*, 10524–10527. [[CrossRef](#)]

61. Wang, Z.; Xu, M.; Zhang, N.; Pan, J.-B.; Wu, X.; Liu, P.; Xu, J.-J.; Hua, D. An ultra-highly sensitive and selective self-enhanced AIECL sensor for public security early warning in a nuclear emergency via a co-reactive group poisoning mechanism. *J. Mater. Chem. A* **2021**, *9*, 12584–12592. [[CrossRef](#)]
62. Wiwasuku, T.; Chuaephon, A.; Habarakada, U.; Boonmak, J.; Puangmali, T.; Kielar, F.; Harding, D.J.; Youngme, S. A water-stable lanthanide-based MOF as a highly sensitive sensor for the selective detection of paraquat in agricultural products. *ACS Sustain. Chem. Eng.* **2022**, *10*, 2761–2771. [[CrossRef](#)]
63. Gao, H.; Wei, X.; Li, M.; Wang, L.; Wei, T.; Dai, Z. Co-quenching effect between lanthanum metal-organic frameworks luminophore and crystal violet for enhanced electrochemiluminescence gene detection. *Small* **2021**, *17*, 2103424. [[CrossRef](#)] [[PubMed](#)]
64. Wang, Y.; Zhao, G.; Chi, H.; Yang, S.; Niu, Q.; Wu, D.; Cao, W.; Li, T.; Ma, H.; Wei, Q. Self-luminescent lanthanide metal-organic frameworks as signal probes in electrochemiluminescence immunoassay. *J. Am. Chem. Soc.* **2021**, *143*, 504–512. [[CrossRef](#)] [[PubMed](#)]
65. Carrara, S.; Arcudi, F.; Prato, M.; De Cola, L. Amine-rich nitrogen-doped carbon nanodots as a platform for self-enhancing electrochemiluminescence. *Angew. Chem. Int. Ed.* **2017**, *56*, 4757–4761. [[CrossRef](#)]
66. Zhu, D.; Zhang, Y.; Bao, S.; Wang, N.; Yu, S.; Luo, R.; Ma, J.; Ju, H.; Lei, J. Dual intrareticular oxidation of mixed-ligand metal-organic frameworks for stepwise electrochemiluminescence. *J. Am. Chem. Soc.* **2021**, *143*, 3049–3053. [[CrossRef](#)]
67. Li, Y.; Cui, W.; Jiang, Q.; Wu, Q.; Liang, R.; Luo, Q.; Qiu, J. A general design approach toward covalent organic frameworks for highly efficient electrochemiluminescence. *Nat. Commun.* **2021**, *12*, 4735. [[CrossRef](#)]
68. Luo, R.; Lv, H.; Liao, Q.; Wang, N.; Yang, J.; Li, Y.; Xi, K.; Wu, X.; Ju, H.; Lei, J. Intrareticular charge transfer regulated electrochemiluminescence of donor-acceptor covalent organic frameworks. *Nat. Commun.* **2021**, *12*, 6808. [[CrossRef](#)]
69. Zhang, N.; Wang, X.; Xiong, Z.; Huang, L.; Jin, Y.; Wang, A.; Yuan, P.; He, Y.; Feng, J. Hydrogen bond organic frameworks as a novel electrochemiluminescence luminophore: Simple synthesis and ultrasensitive biosensing. *Anal. Chem.* **2021**, *93*, 17110–17118. [[CrossRef](#)] [[PubMed](#)]
70. Hou, H.; Wang, Y.; Wang, Y.; Luo, R.; Zhu, D.; Zhou, J.; Wu, X.; Ju, H.; Lei, J. Intrareticular electron coupling pathway driven electrochemiluminescence in hydrogen-bonded organic frameworks. *J. Mater. Chem. C* **2022**, *10*, 14488–14495. [[CrossRef](#)]
71. Ye, F.; Zhao, Y.; El-Sayed, R.; Muhammed, M.; Hassan, M. Advances in nanotechnology for cancer biomarkers. *Nano Today* **2018**, *18*, 103–123. [[CrossRef](#)]
72. Mohammadinejad, A.; Oskuee, R.K.; Eivazzadeh-Keihan, R.; Rezayi, M.; Baradaran, B.; Maleki, A.; Hashemzadeh, M.; Mokhtarzadeh, A.; de la Guardia, M. Development of biosensors for detection of alpha-fetoprotein: As a major biomarker for hepatocellular carcinoma. *TrAC Trends Anal. Chem.* **2020**, *130*, 115961. [[CrossRef](#)]
73. Zhao, C.; Ma, C.; Zhang, F.; Li, W.; Hong, C.; Qi, Y. Two-dimensional metal-organic framework nanosheets: An efficient two-electron oxygen reduction reaction electrocatalyst for boosting cathodic luminol electrochemiluminescence. *Chem. Eng. J.* **2023**, *466*, 143156. [[CrossRef](#)]
74. Li, J.; Lai, W.; Ma, C.; Zhao, C.; Li, P.; Jiang, M.; Wang, M.; Chen, S.; Hong, C. MnO₂ nanosheet/polydopamine double-quenching Ru(bpy)₃²⁺@TMU-3 electrochemiluminescence for ultrasensitive immunosensing of alpha-fetoprotein. *ACS Appl. Nano Mater.* **2022**, *5*, 14697–14705. [[CrossRef](#)]
75. Zhou, L.; Yang, L.; Wang, C.; Jia, H.; Xue, J.; Wei, Q.; Ju, H. Copper doped terbium metal organic framework as emitter for sensitive electrochemiluminescence detection of CYFRA 21-1. *Talanta* **2022**, *238*, 123047. [[CrossRef](#)] [[PubMed](#)]
76. Li, X.; Ren, X.; Yang, L.; Wang, W.; Fan, D.; Kuang, X.; Sun, X.; Wei, Q.; Ju, H. Ru(dcbpy)₃²⁺-functionalized γ -cyclodextrin metal-organic frameworks as efficient electrochemiluminescence tags for the detection of CYFRA21-1 in human serum. *Sens. Actuators B-Chem.* **2023**, *378*, 133152. [[CrossRef](#)]
77. Zhang, P.; Shen, Q.; Wang, J.; Yu, M.; Kang, Q.; Zhang, W.; Zou, G. Intrareticular charge transfer triggered self-electrochemiluminescence of zirconium-based metal-organic framework nanoparticles for potential-resolved multiplex immunoassays with isolated coreactants. *Anal. Chem.* **2023**, *95*, 10096–10104. [[CrossRef](#)]
78. Huang, W.; Hu, G.; Liang, W.; Wang, J.; Lu, M.; Yuan, R.; Xiao, D. Ruthenium(II) complex-grafted hollow hierarchical metal-organic frameworks with superior electrochemiluminescence performance for sensitive assay of thrombin. *Anal. Chem.* **2021**, *93*, 6239–6245. [[CrossRef](#)]
79. Li, P.; Luo, L.; Chen, D.; Sun, Y.; Zhang, Y.; Liu, M.; Yao, S. Regulation of the structure of zirconium-based porphyrinic metal-organic framework as highly electrochemiluminescence sensing platform for thrombin. *Anal. Chem.* **2022**, *94*, 5707–5714. [[CrossRef](#)]
80. Zhang, J.; Yao, L.; Yang, Y.; Liang, W.; Yuan, R.; Xiao, D. Conductive covalent organic frameworks with conductivity- and pre-reduction-enhanced electrochemiluminescence for ultrasensitive biosensor construction. *Anal. Chem.* **2022**, *94*, 3685–3692. [[CrossRef](#)]
81. Xiong, C.; Liang, W.; Zheng, Y.; Zhuo, Y.; Chai, Y.; Yuan, R. Ultrasensitive assay for telomerase activity via self-enhanced electrochemiluminescent ruthenium complex doped metal-organic frameworks with high emission efficiency. *Anal. Chem.* **2017**, *89*, 3222–3227. [[CrossRef](#)]
82. Zhang, H.; Li, B.; Sun, Z.; Zhou, H.; Zhang, S. Integration of intracellular telomerase monitoring by electrochemiluminescence technology and targeted cancer therapy by reactive oxygen species. *Chem. Sci.* **2017**, *8*, 8025–8029. [[CrossRef](#)] [[PubMed](#)]
83. Xu, Z.; Wu, F.; Zhu, D.; Fu, H.; Shen, Z.; Lei, J. BODIPY-based metal-organic frameworks as efficient electrochemiluminescence emitters for telomerase detection. *Chem. Commun.* **2022**, *58*, 11515–11518. [[CrossRef](#)] [[PubMed](#)]
84. Ding, Y.; Zhang, X.; Peng, J.; Zheng, D.; Zhang, X.; Song, Y.; Cheng, Y.; Gao, W. Ultra-sensitive electrochemiluminescence platform based on magnetic metal-organic framework for the highly efficient enrichment. *Sens. Actuators B-Chem.* **2020**, *324*, 128700. [[CrossRef](#)]

85. Zheng, L.; Guo, Q.; Yang, C.; Wang, J.; Xu, X.; Nie, G. Electrochemiluminescence and photoelectrochemistry dual-signal immunosensor based on Ru(bpy)₃²⁺-functionalized MOF for prostate-specific antigen sensitive detection. *Sens. Actuators B* **2023**, *379*, 133269. [[CrossRef](#)]
86. Shao, K.; Wang, B.; Nie, A.; Ye, S.; Ma, J.; Li, Z.; Lv, Z.; Han, H. Target-triggered signal-on ratiometric electrochemiluminescence sensing of PSA based on MOF/Au/G-quadruplex. *Biosens. Bioelectron.* **2018**, *118*, 160–166. [[CrossRef](#)]
87. Li, J.; Yang, H.; Cai, R.; Tang, W. Ultrahighly sensitive sandwich-type electrochemical immunosensor for selective detection of tumor biomarkers. *ACS Appl. Mater. Interfaces* **2022**, *14*, 44222–44227. [[CrossRef](#)]
88. Fang, J.; Dai, L.; Feng, R.; Wu, D.; Ren, X.; Cao, W.; Ma, H.; Wei, Q. High-performance electrochemiluminescence of a coordination driven J-aggregate K-PTC MOF regulated by metal-phenolic nanoparticles for biomarker analysis. *Anal. Chem.* **2023**, *95*, 1287–1293. [[CrossRef](#)]
89. Wang, C.; Li, Z.; Ju, H. Copper-doped terbium luminescent metal organic framework as an emitter and a co-reaction promoter for amplified electrochemiluminescence immunoassay. *Anal. Chem.* **2021**, *93*, 14878–14884. [[CrossRef](#)]
90. Cui, L.; Zhu, C.; Hu, J.; Meng, X.; Jiang, M.; Gao, W.; Wang, X.; Zhang, C. Construction of a dual-mode biosensor for electrochemiluminescent and electrochemical sensing of alkaline phosphatase. *Sens. Actuators B* **2023**, *374*, 132779. [[CrossRef](#)]
91. Zhao, J.; Du, Y.; Zhang, N.; Li, C.; Ma, H.; Wu, D.; Cao, W.; Wang, Y.; Wei, Q. Dual-quenching mechanisms in electrochemiluminescence immunoassay based on zinc-based MOFs of ruthenium hybrid for D-dimer detection. *Anal. Chim. Acta* **2023**, *1253*, 341076. [[CrossRef](#)] [[PubMed](#)]
92. Liu, Q.; Huang, Y.; Li, Z.; Li, L.; Zhao, Y.; Li, M. An enzymatically gated catalytic hairpin assembly delivered by lipid nanoparticles for the tumor-specific activation of signal amplification in miRNA imaging. *Angew. Chem. Int. Ed.* **2022**, *61*, e202214230.
93. Yao, Q.; Wang, Y.; Wang, J.; Chen, S.; Liu, H.; Jiang, Z.; Zhang, X.; Liu, S.; Yuan, Q.; Zhou, X. An ultrasensitive diagnostic biochip based on biomimetic periodic nanostructure-assisted rolling circle amplification. *ACS Nano* **2018**, *12*, 6777–6783. [[CrossRef](#)]
94. Wei, J.; Wang, H.; Wu, Q.; Gong, X.; Ma, K.; Liu, X.; Wang, F. A Smart, Autocatalytic, DNAzyme biocircuit for in vivo, amplified, microRNA imaging. *Angew. Chem. Int. Ed.* **2020**, *59*, 5965–5971. [[CrossRef](#)]
95. Liu, Y.; Wang, F.; Ge, S.; Zhang, L.; Zhang, Z.; Liu, Y.; Zhang, Y.; Ge, S.; Yu, J. Programmable T-junction structure-assisted CRISPR/Cas12a electrochemiluminescence biosensor for detection of Sa-16S rDNA. *ACS Appl. Mater. Interfaces* **2023**, *15*, 617–625. [[CrossRef](#)]
96. Hill, M.; Tran, N. MicroRNAs regulating microRNAs in cancer. *Trends Cancer* **2018**, *4*, 465–468. [[CrossRef](#)]
97. Wang, X.; Wang, X.; Hu, C.; Guo, W.; Wu, X.; Chen, G.; Dai, W.; Zhen, S.; Huang, C.; Li, Y. Controlled synthesis of zinc-metal organic framework microflower with high efficiency electrochemiluminescence for miR-21 detection. *Biosens. Bioelectron.* **2022**, *213*, 114443. [[CrossRef](#)]
98. Xue, Y.; Liao, N.; Li, Y.; Liang, W.; Yang, X.; Zhong, X.; Zhuo, Y. Ordered heterogeneity in dual-ligand MOF to enable high electrochemiluminescence efficiency for bioassay with DNA triangular prism as signal switch. *Biosens. Bioelectron.* **2022**, *217*, 114713. [[CrossRef](#)]
99. Yin, T.; Wu, D.; Du, H.; Jie, G. Dual-wavelength electrochemiluminescence biosensor based on a multifunctional Zr MOFs@PEI@AuAg nanocomposite with intramolecular self-enhancing effect for simultaneous detection of dual microRNAs. *Biosens. Bioelectron.* **2022**, *217*, 114699. [[CrossRef](#)]
100. Wei, Y.; Chen, J.; Liu, X.; Miao, C.; Jin, B. ORAOV 1 detection made with metal organic frameworks based on Ti₃C₂T_x MXene. *ACS Appl. Mater. Interfaces* **2022**, *14*, 23726–23733. [[CrossRef](#)]
101. Yang, Y.; Zhang, J.; Liang, W.; Zhang, J.; Xu, X.; Zhang, X.; Yuan, R.; Xiao, D. Conductive NiCo bimetal-organic framework nanorods with conductivity-enhanced electrochemiluminescence for constructing biosensing platform. *Sens. Actuators B* **2020**, *362*, 131802. [[CrossRef](#)]
102. Zhang, J.; Yang, Y.; Liang, W.; Yao, L.; Yuan, R.; Xiao, D. Highly stable covalent organic framework nanosheets as a new generation of electrochemiluminescence emitters for ultrasensitive microRNA detection. *Anal. Chem.* **2021**, *93*, 3258–3265. [[CrossRef](#)]
103. Musso, D.; Gubler, D.J. Zika Virus. *Clin. Microbiol. Rev.* **2016**, *29*, 487–524. [[CrossRef](#)]
104. Zhang, Y.; Liu, W.; Chen, J.; Niu, H.; Mao, C.; Jin, B. Metal-organic gel and metal-organic framework based switchable electrochemiluminescence RNA sensing platform for Zika virus. *Sens. Actuators B-Chem.* **2020**, *321*, 128456. [[CrossRef](#)]
105. Li, Y.; Li, J.; Zhu, D.; Wang, J.; Shu, G.; Li, J.; Zhang, S.; Zhang, X.; Cosnier, S.; Zeng, H.; et al. 2D Zn-porphyrin-based Co(II)-MOF with 2-methylimidazole sitting axially on the paddle-wheel units: An efficient electrochemiluminescence bioassay for SARS-CoV-2. *Adv. Funct. Mater.* **2022**, *32*, 2209743. [[CrossRef](#)]
106. Wu, D.; Dong, W.; Yin, T.; Jie, G.; Zhou, H. PCN-224/nano-zinc oxide nanocomposite-based electrochemiluminescence biosensor for HPV-16 detection by multiple cycling amplification and hybridization chain reaction. *Sens. Actuators B-Chem.* **2022**, *372*, 132659. [[CrossRef](#)]
107. Li, J.; Luo, M.; Jin, C.; Zhang, P.; Yang, H.; Cai, R.; Tan, W. Plasmon-enhanced electrochemiluminescence of PTP-decorated Eu MOF-based Pt-tipped Au bimetallic nanorods for the lincomycin assay. *ACS Appl. Mater. Interfaces* **2022**, *14*, 383–389. [[CrossRef](#)]
108. Li, J.; Luo, M.; Yang, H.; Ma, C.; Cai, R.; Tan, W. Novel dual-signal electrochemiluminescence aptasensor involving the resonance energy transform system for kanamycin detection. *Anal. Chem.* **2022**, *94*, 6410–6416. [[CrossRef](#)]
109. Wang, J.; Xu, X.; Zheng, L.; Guo, Q.; Nie, G. A signal “on-off-on”-type electrochemiluminescence aptamer sensor for detection of sulfadimethoxine based on Ru@Zn-oxalate MOF composites. *Microchim. Acta* **2023**, *190*, 131. [[CrossRef](#)]
110. Shen, K.; Zhang, J.; Shen, L.; Xiong, Z.; Zhu, H.; Wang, A.; Yuan, P.; Feng, J. Hydrogen bond organic frameworks as radical reactors for enhancement in ECL efficiency and their ultrasensitive biosensing. *Anal. Chem.* **2023**, *95*, 4735–4743. [[CrossRef](#)]

111. Wang, B.; Zhao, L.; Li, Y.; Liu, X.; Fan, D.; Wu, D.; Wei, Q. Porphyrin-based metal-organic frameworks enhanced electrochemiluminescence (ECL) by overcoming aggregation-caused quenching: A new ECL emitter for the detection of trenbolone. *Anal. Chim. Acta* **2023**, *1276*, 341616. [[CrossRef](#)]
112. Tao, X.; Pan, C.; Yang, X.; Yuan, R.; Zhuo, Y. CDs assembled metal-organic framework: Exogenous coreactant-free biosensing platform with pore confinement-enhanced electrochemiluminescence. *Chin. Chem. Lett.* **2022**, *33*, 4803–4807. [[CrossRef](#)]
113. Nie, Y.; Tao, X.; Zhang, H.; Chai, Y.; Yuan, R. Self-assembly of gold nanoclusters into a metal-organic framework with efficient electrochemiluminescence and their application for sensitive detection of rutin. *Anal. Chem.* **2021**, *93*, 3445–3451. [[CrossRef](#)] [[PubMed](#)]
114. Zheng, H.; Yi, H.; Dai, H.; Fang, D.; Hong, Z.; Lin, D.; Zheng, X.; Lin, Y. Fluoro-coumarin silicon phthalocyanine sensitized integrated electrochemiluminescence bioprobe constructed on TiO₂ MOFs for the sensing of deoxynivalenol. *Sens. Actuators B-Chem.* **2018**, *269*, 27–35. [[CrossRef](#)]
115. An, X.; Jiang, D.; Cao, Q.; Xu, F.; Shiigi, H.; Wang, W.; Chen, Z. Highly efficient dual-color luminophores for sensitive and selective detection of diclazepam based on MOF/COF bi-mesoporous composites. *ACS Sens.* **2023**. [[CrossRef](#)]
116. Shan, X.; Pan, T.; Pan, Y.; Wang, W.; Chen, X.; Shan, X.; Chen, Z. Highly sensitive and selective detection of Pb (II) by NH₂SiO₂/Ru(bpy)₃²⁺ UiO66 based solid-state ECL sensor. *Electroanalysis* **2020**, *32*, 462–469. [[CrossRef](#)]
117. He, Q.-N.; Ma, Z.-Y.; Yang, Y.-X.; Xu, C.-H.; Zhao, W. Recent advances in electrochemiluminescence-based single-cell analysis. *Chemosensors* **2023**, *11*, 281. [[CrossRef](#)]
118. Pan, D.; Fang, Z.; Yang, E.; Ning, Z.; Zhou, Q.; Chen, K.; Zheng, Y.; Zhang, Y.; Shen, Y. Facile preparation of WO_{3-x} dots with remarkably low toxicity and uncompromised activity as co-reactants for clinical diagnosis by electrochemiluminescence. *Angew. Chem. Int. Ed.* **2020**, *59*, 16747–16754. [[CrossRef](#)]
119. Ding, H.; Zhou, P.; Fu, W.; Ding, L.; Guo, W.; Su, B. Spatially selective imaging of cell-matrix and cell-cell junctions by electrochemiluminescence. *Angew. Chem. Int. Ed.* **2021**, *60*, 11769–11773. [[CrossRef](#)]
120. Li, B.; Huang, X.; Lu, Y.; Fan, Z.; Li, B.; Jiang, D.; Sojic, N.; Liu, B. High electrochemiluminescence from Ru(bpy)₃²⁺ embedded metal-organic frameworks to visualize single molecule movement at the cellular membrane. *Adv. Sci.* **2022**, *9*, 2204715. [[CrossRef](#)]
121. Wei, W.; Lin, H.; Shao, H.; Hao, T.; Wang, S.; Hu, Y.; Guo, Z.; Su, X. Faraday cage-type aptasensor for dual-mode detection of *Vibrio parahaemolyticus*. *Microchim. Acta* **2020**, *187*, 529. [[CrossRef](#)] [[PubMed](#)]
122. Sun, Y.; Chen, Y.; Duan, Y.; Ma, F. Electrogenated chemiluminescence biosensor based on functionalized two-dimensional metal-organic frameworks for bacterial detection and antimicrobial susceptibility assays. *ACS Appl. Mater. Interfaces* **2021**, *13*, 38923–38930. [[CrossRef](#)]
123. Wang, Y.; Shu, J.; Lyu, A.; Wang, M.; Hu, C.; Cui, H. Zn²⁺-modified nonmetal porphyrin-based metal-organic frameworks with improved electrochemiluminescence for nanoscale exosome detection. *ACS Appl. Nano Mater.* **2023**, *6*, 4214–4223. [[CrossRef](#)]
124. Liang, T.; Guo, Z.; He, Y.; Wang, Y.; Li, C.; Li, Z.; Liu, Z. Cyanine-doped lanthanide metal-organic frameworks for near-infrared II bioimaging. *Adv. Sci.* **2022**, *9*, 2104561. [[CrossRef](#)]
125. Liu, Y.; Zhang, H.; Li, B.; Liu, J.; Jiang, D.; Liu, B.; Sojic, N. Single biomolecule imaging by electrochemiluminescence. *J. Am. Chem. Soc.* **2021**, *143*, 17910–17914. [[CrossRef](#)] [[PubMed](#)]
126. Deneff, J.I.; Rohwer, L.E.S.; Butler, K.S.; Kaehr, B.; Vogel, D.J.; Luk, T.S.; Reyes, R.A.; Cruz-Cabrera, A.A.; Martin, J.E.; Sava Gallis, D.F. Orthogonal luminescence lifetime encoding by intermetallic energy transfer in heterometallic rare-earth MOFs. *Nat. Commun.* **2023**, *14*, 981. [[CrossRef](#)]
127. Ji, Z.; Li, T.; Yaghi, O.M. Sequencing of metals in multivariate metal-organic frameworks. *Science* **2020**, *369*, 674–680. [[CrossRef](#)]
128. Qin, X.; Zhan, Z.; Ding, Z. Progress in electrochemiluminescence biosensors based on organic framework emitters. *Curr. Opin. Electrochem.* **2023**, *39*, 101283. [[CrossRef](#)]

Disclaimer/Publisher's Note: The statements, opinions and data contained in all publications are solely those of the individual author(s) and contributor(s) and not of MDPI and/or the editor(s). MDPI and/or the editor(s) disclaim responsibility for any injury to people or property resulting from any ideas, methods, instructions or products referred to in the content.